

# Frequency and trends in cold and warm spells in Norway in relation to large-scale atmospheric circulation

Marek Grzegorz Ratajczak



Thesis submitted for the degree of  
Master in Meteorology and Oceanography  
60 credits

Department of Geosciences  
The Faculty of Mathematics and Natural Sciences

UNIVERSITY OF OSLO

Autumn 2020



**Frequency and trends in cold  
and warm spells in Norway in  
relation to large-scale  
atmospheric circulation**

Marek Grzegorz Ratajczak

© 2020 Marek Grzegorz Ratajczak

Frequency and trends in cold and warm spells in Norway in relation to  
large-scale atmospheric circulation

<http://www.duo.uio.no/>

Printed: Representralen, University of Oslo

# Abstract

Periods of unusually high or low temperatures have a significant impact on both nature and society at all times of the year. A possible change in frequency or persistence of such events would impact the wildlife as well as the economy and people's everyday life. In Norway, a major factor determining temperature anomalies is the large-scale atmospheric circulation. It is therefore of interest to examine frequency and length of both cold/warm spells and certain circulation patterns in order to find a possible connection between trends. In the following study, it is done by analyzing daily minimum and maximum temperature from 1979 to 2018 measured at selected stations owned by the Norwegian Meteorological Institute and applying different classification methods included in cost733class software on daily mean sea level pressure from ERA5 global reanalysis for the same time period.

The results show that both frequency and length of cold and warm spells during winter (October to March) and summer (April to September), defined as a number of consecutive days with minimum/maximum temperature below the 25th/above the 75th percentile, have changed during the last four decades at all locations, with an overall increase in both measures for warm spells during both seasons and an overall decrease in both measures for cold spells during both seasons, with exception of the length of cold spells in winter which are varying between locations. By looking at relative frequency of different circulation types during cold and warm spells, as well as average temperatures measured during each circulation type, circulation types associated with these spells are identified. Warm spells are generally associated with air flow from southerly directions, while cold spells are associated with air flow from northerly directions. Air masses of continental origin in the east contribute to warm spells in summer and cold spells in winter, while the opposite is true for maritime air masses to the west. Further analysis indicates that circulation types responsible for cold spells have got slightly less frequent, while circulation types resulting in warm spells have got slightly more frequent, which would contribute to the change in frequency of observed cold and warm spells. Still, the magnitude of change is larger for the actual spells than for the atmospheric circulation, so a dominating factor would be that the temperature has increased everywhere for almost every circulation type, increasing the probability of the occurrence of warm spells and lowering it for cold spells.

# Contents

<b>1</b>	<b>Introduction</b>	<b>1</b>
<b>2</b>	<b>Background</b>	<b>2</b>
2.1	Circulation of the troposphere . . . . .	2
2.2	Circulation type classification . . . . .	3
2.3	Climate in Norway . . . . .	3
<b>3</b>	<b>Data</b>	<b>6</b>
3.1	Observational data . . . . .	6
3.2	Reanalysis data . . . . .	9
<b>4</b>	<b>Methodology</b>	<b>10</b>
4.1	Classification of circulation . . . . .	10
4.2	Cold and warm spells . . . . .	10
4.3	Relationship between cold/warm spells and circulation types	12
<b>5</b>	<b>Results</b>	<b>13</b>
5.1	Cold and warm spell trends . . . . .	13
5.2	Cold and warm spells and large-scale circulation relationship	16
5.3	Large-scale circulation trends . . . . .	27
<b>6</b>	<b>Discussion</b>	<b>33</b>
<b>7</b>	<b>Summary and outlook</b>	<b>37</b>
<b>A</b>	<b>Appendix</b>	<b>40</b>

# Dedication

Ku pamięci mojego ojca, Jana Ratajczaka, który odszedł nieoczekiwanie zaledwie kilka miesięcy przed ukończeniem mojej pracy magisterskiej. Mimo, że nie mogłeś dożyć tego dnia to wiem, że zawsze we mnie wierzyles i cieszyles się tym, że realizuję swoje marzenia.

In memory of my father, Jan Ratajczak, who left us abruptly only a few months before I could finalize my master's thesis. Even though you could not live to see this day, I know you always had faith in me and was happy that I am following my dreams.

# Acknowledgements

I would like to thank Ole Einar Tveito, Malte Müller and Oskar Landgren, my supervisors, for helping me work on my thesis, from formal and technical matters to scientific support. Most of all I want to thank them for not giving up on me even when working on this thesis seemed impossible to me.

Moreover, I want to thank my mother and brother, Mirosława and Paweł Ratajczak, for showing their understanding for decisions I had to make in the past few months.

I also want to thank my friend, Jesper Schildger, for keeping me sane during months of societal restrictions due to COVID-19 pandemic.

Lastly, I wanted to thank my coworkers from the time I worked in the warehouse at Mascot Høie for helping me find the trust in my own abilities and find the courage to continue the Master's studies.



# Chapter 1

## Introduction

Spells of unusually high or low temperatures which last for many consecutive days have a significant impact on both nature and society at all times of the year. Extreme cold during the winter leads to higher power usage for heating and may cause freezing of the water pipes and thus their damage. Wildlife as well as agriculture highly depends on temperature during spring, when a warm type of weather may result in an early start of the growth season, while low temperatures will put a delay on that start or even damage the crops. Summer heat waves may still not be as life threatening in Norway as they are further south, but they still cause higher evaporation rate of water which may lead to drought, deficit of drinking water and water as a source of hydroelectric power, as well as higher risk of forest fires. Both persistence and frequency of such events are therefore of matter where a change in either of those measures does not come without consequences for the economy as well as for the natural and social life.

The objective of the first part of this analysis is to determine whether there has been a significant change in persistence and/or frequency of cold and warm spells in a selection of different locations in Norway during the last four decades. The objective of the second part of this analysis is to determine whether there has been a significant change in persistence and/or frequency of occurrence of atmospheric circulation types associated with previously determined cold and warm spells during the same time period. The final objective is to determine whether the change in persistence and/or frequency of cold and warm spells can be explained by a change in the large-scale circulation in Northern Europe.

## Chapter 2

# Background

### 2.1 Circulation of the troposphere

The Earth's atmosphere is a dynamic system affected by factors such as Earth's rotation, uneven solar heating, chemical reactions between atmospheric gases, biological processes on the surface and anthropogenic activity. The motion of that system is referred to as the atmospheric circulation and its purpose is to distribute the thermal energy around the globe. The large-scale atmospheric circulation, i.e. systems of high and low pressure on a size scale of hundreds of kilometers (cyclones and anticyclones) is mainly driven by the Earth's rotation and temperature differences. The temperature differences between the tropics and the poles cause meridional air transport, while the Earth's rotational motion together with its curvature tend to change the direction of that transport to the right in the northern hemisphere and to the left in the southern hemisphere, a phenomenon known as the Coriolis force.

The large scale atmospheric circulation and its variations is therefore the driving force for determining regional and local climate. In the extratropics, the large-scale atmospheric circulation plays an important role in the weather formation, especially during the winter when solar heating is low. The constantly moving and changing pressure systems can change the weather at one location diametrically from day to day. Even though the atmosphere is quite chaotic, there are still some prevailing patterns, e.g. trade winds in the tropics (northeasterly in the northern hemisphere, southeasterly in the southern hemisphere) and westerly winds in mid-latitudes. Other, less regular phenomena, are El Niño-Southern Oscillation (ENSO) or North Atlantic Oscillation (NAO). ENSO is characterized by changes in the tropical trade winds and the sea surface temperature in the eastern Pacific Ocean. These changes have a huge impact on the weather and climate of the tropics and the Pacific region. NAO ([1]) is defined as the pressure difference between Iceland and Azores and is an indicator of how strong the westerly winds in the North Atlantic are. The weather in large parts of Europe, as well as in eastern North America, Mediterranean coast of Africa and parts of the Middle East is affected by variations in the NAO index.

## 2.2 Circulation type classification

Classification is in principle an attempt to simplify, and thus achieve a better understanding of complex systems. The atmosphere is such a system, and there is a long tradition for categorizing weather system in to specific circulation types, weather types or circulation patterns. The most well-known classifications are the subjective manual classifications Grosswetterlagen for central Europe by Hess and Brezowski ([8]) and the Lamb weather types for the British Isles([4]).

During the last decades automatic methods for atmospheric circulation classification have been developed. There are several concepts for classifying atmospheric circulation([3]), based on different methodological approaches. A joint European effort, the COST733 Action "Harmonisation and Applications of Weather Types Classifications for European Regions" compared and evaluated several different methods for various applications ([7]). COST733 divided the automatic classification methods in categories based on their concepts:

- predefined types, including automated algorithms for the grosswetterlagen and Lambs weather types.
- eigenvector based methods, based on e.g. principal components.
- leader algorithms, often based on correlation or covariance structures.
- optimization algorithms, such as cluster analysis algorithms.

The COST733 -action developed a software ([6]) including a large number of automated methods that provide objective and consistent classifications of atmospheric circulation. In this analysis are some of these, representing different classification principles selected in order to study trends in local cold and warm spells and their relation to large scale atmospheric circulation.

## 2.3 Climate in Norway

Norway, being located in the northern part of Europe, is influenced by the mid-latitude atmospheric dynamics with prevailing westerly winds. Because of that, and the fact that Norway is bordering the North Sea and the Norwegian Sea to the west, the climate is relatively mild with small temperature differences throughout the year along the coast. In addition, large parts of the country are covered by mountains with an altitude exceeding 2000 m.a.s.l. in the south, 1500 m.a.s.l. in the north and slightly lower in the central part, which makes the Norwegian coast one of the wettest places in Europe. Another consequence of the mountainous topography is adiabatic warming of the air on the lee-side of the mountains after the moist air has been lifted and the water is precipitated, also known as the foehn wind. Inland parts of Norway, both in the south (east of the

watershed) and the north (the Finnmark Plateau) are rather dry with cold winters and warm summers.

Although the westerly winds are dominating, other atmospheric circulation patterns contribute to high variability in the weather and climate. Circulation blocking, associated with a negative NAO index, results in dry conditions and clear sky on both sides of mountains, followed by low temperatures during the winter and high temperatures in the summer. Air flow from northerly directions brings cold air from the high Arctic and results in frequent showers along the coast, while air flowing from the south cause exceptionally high temperatures in the valleys and fjords of northern part of the west coast.

To exemplify how different atmospheric circulation patterns lead to extreme temperatures in Norway during different seasons, Figure 2.1 shows mean sea level pressure for selected months in the last decade. November 2010 was (together with Nov 1919) the coldest November ever recorded in Norway. As shown on the map, there was a high pressure system located over northern Sweden and a belt of weak low pressure system stretching from the British Isles to southern border of the Baltic Sea, together transporting cold and dry air masses from northern Russia. In contrast, January 2020 was the second warmest January on record in Norway. The air was flowing straight from the Atlantic Ocean, and the high density of the isobars means a strong flow. June 2015 was one of the colder Junes and the map showing a low pressure system outside of the Kola Peninsula indicates that there was a frequent flow of air from the Arctic Ocean in the north. Lastly, July 2014 was the warmest July ever recorded in Norway (later tied by July 2018). There were two high pressure systems - one above the Azores and the other one close to the Kola Peninsula - with a ridge between. That combined resulted in a weak flow of air from southern Russia.

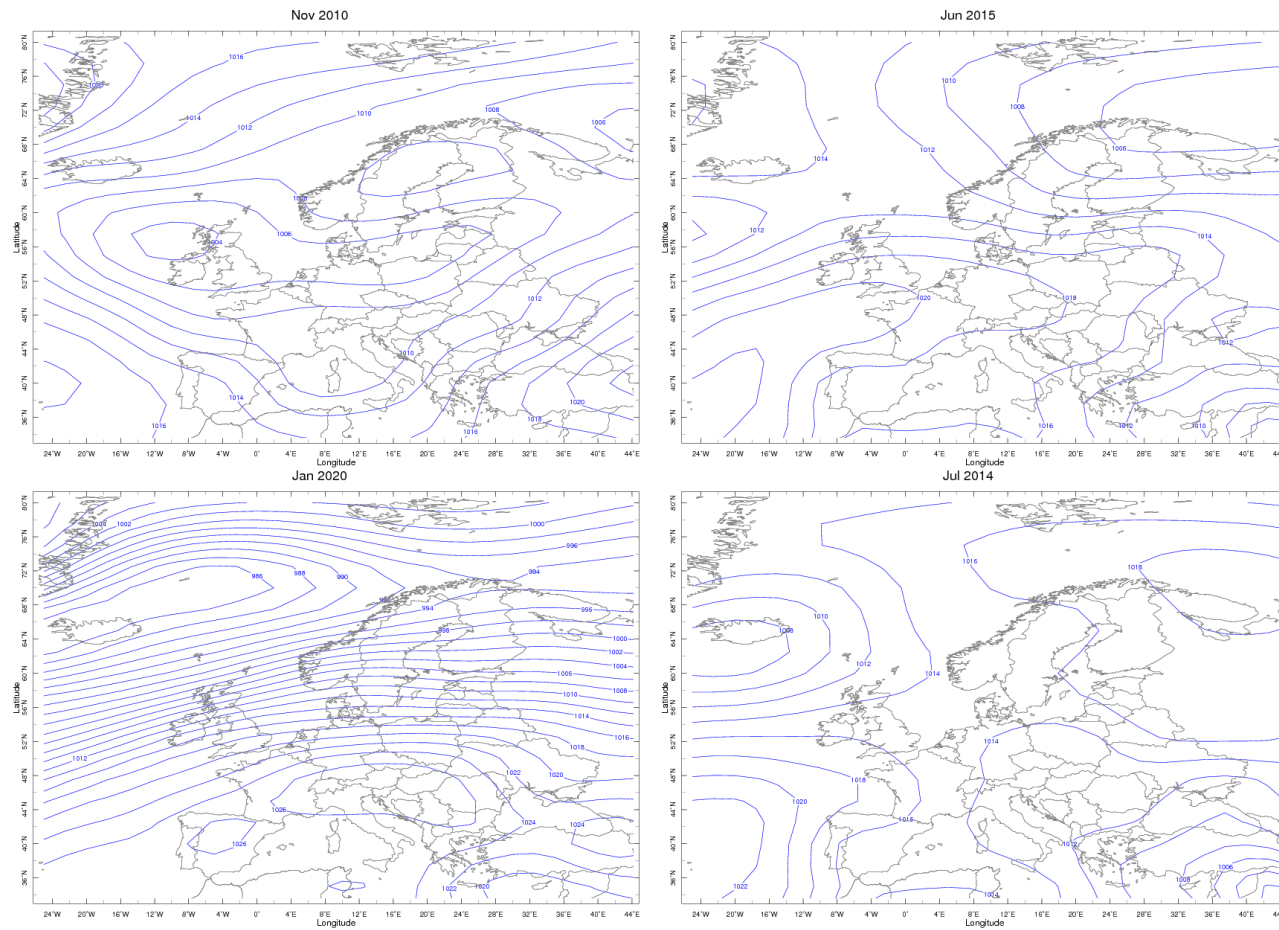


Figure 2.1: Monthly-mean sea level pressure for selected months with extreme temperature anomalies in Norway. Top: extreme cold. Bottom: extreme warm.

# Chapter 3

## Data

### 3.1 Observational data

Observational data from the Norwegian Meteorological Institute used in this analysis includes daily measurements of minimum temperature (TAN) and maximum temperature (TAX) measured 2 m above the ground level during the period 1.1.1979 - 31.12.2018 for six different locations in Norway. At some locations the observation point has been moved during that period. That could have an impact on the observations caused by local conditions (altitude, exposure to wind, albedo of surroundings), although the new locations are so close to the old ones that the impact on the observations continuity should be negligible. Additionally, some data is missing for most of the locations, ranging from a few days up to almost two years in total (see Table 3.1).

Six different locations are chosen to represent different regions in Norway: Eastern Norway (Oslo and Drevsjø), Western Norway (Bergen), Central Norway/Trøndelag (Ørland) and Northern Norway (Tromsø and Karasjok). Large-scale circulation patterns have different impacts on those regions, both because of large distance from north to south (more than 1000 km from Oslo and Bergen to Tromsø and Karasjok), comparable to the size of large-scale weather systems, and also due to topography and location relative to the coast.

Another reason for choosing those locations is to show differences between coastal climate with small temperature differences and frequent precipitation (Bergen, Ørland and Tromsø) and more continental climate with large temperature differences, low precipitation and frequent temperature inversion (Drevsjø, Karasjok). For Oslo, influenced by both coastal and continental climate, measurements from two different points are used: Blindern, right outside of the city centre, and Tryvannshøgda, the top of a hill about 6 km from Blindern. The elevation at Tryvannshøgda is 420 m higher than Blindern. During the cold season (October - March), Oslo experiences frequent temperature inversion under the regime of high pressure systems or during passing of warm fronts, meaning that cold periods can both be lasting for a longer period of time and be more intense.

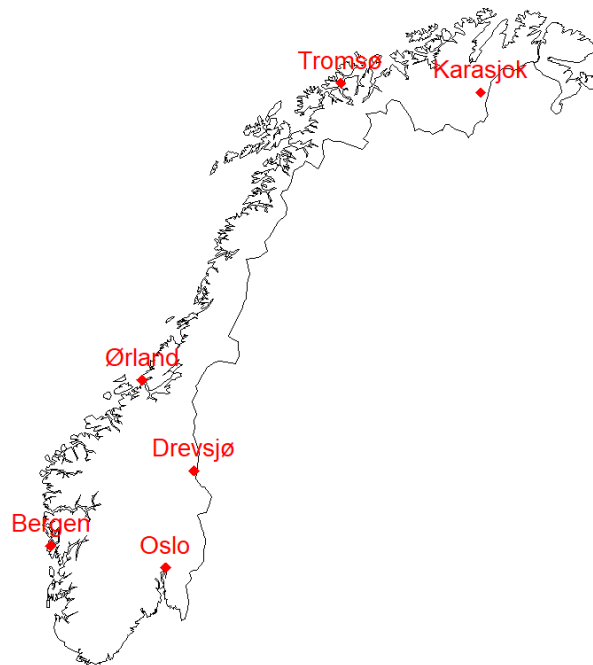


Figure 3.1: All locations used in the analysis marked on the map of Norway.

Location	Station nr and name	from date - to date	Elevation (a.s.l.) lat, lon	Comments
Oslo - Blindern (BLI)	18700 OSLO-BLINDERN	01.01.79 - 31.12.18	94 m 59.9423 N, 10.7200 E	Full data coverage.
Oslo - Tryvannshøgda (TRY)	18960 TRYVASSHØGDA II	01.01.79 - 30.06.97	528 m 59.9886 N, 10.6678 E	Missing data for 01.12.00 - 30.04.02 and some other shorter periods. Total missing 675 days of TAN and 680 days of TAX.
	18950 TRYVANNSHØGDA	01.07.97 - 31.12.18	514 m 59.9847 N, 10.6693 E	
Drevsjø (DRE)	700 DREVSJØ	01.01.79 - 31.12.18	672 m 59.9847 N, 10.6693 E	Missing data for 3 months in 1987 and 2002, as well as a few other days. Total missing 284 days of TAN and TAX.
BERGEN (BER)	50540 BERGEN-FLORIDA	01.01.79 - 31.12.18	12 m 60.3830 N, 5.3327 E	Full data coverage.
Ørland (ØRL)	71550 ØRLAND III	01.01.79 - 31.12.18	10 m 63.7045 N, 9.6105 E	Missing 10 days of TAN and 12 days of TAX.
Tromsø (TRO)	90450 TROMSØ	01.01.79 - 17.01.06	100 m 69.6542 N, 18.9369 E	Missing 3 days of TAN and TAX.
		17.01.06 - 31.12.18	100 m 69.6537 N, 18.9368 E	
Karasjok (KAR)	97250 KARASJOK 97251 KARASJOK-MARKANNJARGA	01.01.79 - 31.08.04	129 m 69.4670 N, 25.5030 E	Missing 2 days of TAN and 1 day of TAX.
		01.09.04 - 31.12.18	131 m 69.4635 N, 25.5023 E	

Table 3.1: Metadata for stations used.



## 3.2 Reanalysis data

For classification of circulation types, atmospheric sea level pressure from the global reanalysis ERA5 ([2]) from the European Centre for Medium Range Weather Forecasts (ECMWF) was used. The spatial domain was chosen to be between 20°W and 40°E with 4° resolution in longitudinal direction and between 40°N and 80°N with 2° resolution in latitudinal direction. To obtain daily values for each grid point, values at 18, 00, 06 and 12 UTC (in that order) were averaged in order to follow the convention used by the Norwegian Meteorological Institute for measuring temperature, where a day starts at 18 UTC on the previous day. As an example, in order to get the pressure value for 2 January 1979, an average of values at 18 UTC on 1 January 1979 and 00, 06 and 12 UTC on 2 January 1979 was calculated. The reanalysis data cover the time period 1 January 1979 to 1 January 2019.

# Chapter 4

## Methodology

### 4.1 Classification of circulation

The classification of circulation types is done applying different methods provided by the `cost733class` software [6]. The classification methods included in the software are divided into some main categories, such as pre-defined types, eigenvector-based methods, leading algorithms and optimization methods. At least one method from each category is chosen to see whether some methods are performing better than others for different locations and different seasons. For each method used, the circulation is classified into 9-10 different types. Further on, for each method, each day in the time series is assigned a number indicating the circulation type given by the software. The applied classification methods are listed in table 4.1.

### 4.2 Cold and warm spells

For this analysis, the year is split in two seasons, each starting close to the equinox. For simplicity the winter season is starting on October 1 and ending on March 31, while the summer season is going on from April 1 to September 30. The reason to do so is to differentiate between the time when solar heating has a large direct impact on the dynamics of the atmosphere and local weather in Northern Europe and the time when that impact is low.

To eliminate the seasonality of both the average temperature and the temperature deviation from the average, temperature thresholds are calculated for each day of the year separately instead of using one threshold value for the absolute temperature or one value for the anomaly from a climatological average. This is done by finding the empirical distribution function (EDF) for each day of the year. The function for the  $n$ -th day of the year is found by using all days in the interval  $[n - 15, n + 15]$  for all years in the 1979–2018 period. For example, to find the EDF for TAN on the first day of the year (January 1), TANs for all days between (and including) December 17 and January 16 for all years between (and including) 1979 and 2018 are used. Later on, the EDFs are used to converse measured temperatures into probabilities, i.e. for finding the probability of TAN not

Name	No. of types	Method
GWT	10	<i>Predefined types</i> based on three prototype fields. Works only with fixed classes, and when applying ten types the circulation types represent the eight main wind directions (N, NE, E, E, SE, S, SW, W, NW) plus pure cyclonic and pure anticyclonic situations.
PTT	9	<i>Eigenvector method</i> . It is a t-mode principal component analysis with orthogonal rotation.
LND	9	Leader algorithm method based on pattern correlations
PXE	10	<i>Eigenvector method</i> Extreme score method applying principal components
KMN	9	Optimization algorithm based on a k-means cluster analysis. The number of classes $k$ is determined by the user. Starting pattern is selected by random
SAN	9	Builds on the same principles as k-means, but is usually more effective due to a different randomization algorithm.

Table 4.1: Methods used for circulation type classification. More details are given by [5] and [3].

exceeding the TAN measured on 1 January 1979, the previously found EDF for January 1 is used. This is done for each location separately.

A cold spell is then defined as a period of at least  $s$  consecutive days with TAN below the 25th percentile threshold, where 1 out of  $s$  consecutive days within that period of time is allowed to be above the threshold as long as it is not the first or the last day of that cold spell. Similarly, a warm spell is defined as a period of at least  $s$  consecutive days with TAN above the 75th percentile threshold, where 1 out of  $s$  consecutive days within that period of time is allowed to be below the threshold as long as it is not the first or the last day of that warm spell. The main focus is on spells with length of 7 days or longer ( $s = 7$ ), but short spells ( $s = 5$ ) and long spells ( $s = 10$ ) are compared as well. As a consequence, a time period of 11 days where TAN at the 5th and the 10th day is above the 25th percentile and else below would be included as a short spell ( $\geq 5$  days), but not as longer spells (neither  $\geq 10$  days nor  $\geq 7$  days).

### 4.3 Relationship between cold/warm spells and circulation types

In order to identify which circulation types (CT) are connected to the cold/warm spells, relative frequency of  $CT_i$  is introduced:

$$freq_i = \frac{CT_i}{\sum_{i=1}^t CT_i} = \frac{CT_i}{N}$$

where  $CT_i$  is number of occurrences of circulation type number  $i$ ,  $t$  is number of CTs for a given classification method and  $N$  is total number of days.

Then, the change between relative frequency of  $CT_i$  during cold (or warm) spells,  $freq_{i, spell}$ , and relative frequency of  $CT_i$  during the entire season,  $freq_{i, season}$  is calculated:

$$freq_{i, change} = freq_{i, spell} - freq_{i, season}$$

If  $freq_{i, change}$  is significantly greater than zero, the CT number  $i$  is chosen to be associated with cold (or warm) spells. Such sets of CTs are depending on the classification method, season and location.

In addition, annual mean temperatures are calculated for each location and each CT in order to find temperature trends for each CT separately and to show which temperatures can be expected during different CTs.

# Chapter 5

## Results

### 5.1 Cold and warm spell trends

Figure 5.1 shows the number of spells of each type and each season at three different locations for every year, as well as trends calculated using linear regression. The other four locations are shown in the Appendix in Figure A.1. Notice that short spells ( $\geq 5$  days) also can last longer than 10 days, although they do not necessarily overlap with  $\geq 10$  day spells (see Section 4.2). In addition, Table 5.1 shows average yearly numbers of spells together with trend values and their significance for spells lasting 7 days or longer. Most frequent are cold spells in winter and warm spells in summer, while cold spells in summer are the least frequent. The longest spells ( $\geq 10$  days) are also less frequent at DRE and KAR, both being located inland. Although there are some large interannual variations, most cases have experienced significant changes in frequency in the course of four decades. Overall, frequency of cold spells of all lengths is decreasing everywhere both during winter and summer, while frequency of warm spells is increasing. The rate of change in time is in most cases higher for shorter spells, which is showing best for cold spells in summer - in many cases the frequency is decreasing by more than 1 spell per year per decade. It is worth noticing that cold spells lasting 10 days or longer are almost not occurring during summer after year 2000 anywhere.

	winter, cold	winter, warm	summer, cold	summer, warm
BLI	2.5 (-0.44)	2.2 (0.14)	1.5 ( <b>-0.73</b> )	2.5 ( <b>0.51</b> )
TRY	2.4 ( <b>-0.59</b> )	2.2 (0.30)	1.6 ( <b>-0.76</b> )	2.5 (0.34)
DRE	2.2 (-0.39)	1.7 (0.24)	2.0 ( <b>-0.68</b> )	2.5 ( <b>0.44</b> )
BER	2.5 (-0.03)	2.2 (0.30)	1.8 ( <b>-0.83</b> )	2.6 ( <b>0.77</b> )
ØRL	2.6 (-0.37)	2.0 ( <b>0.59</b> )	2.1 ( <b>-0.80</b> )	2.2 ( <b>0.80</b> )
TRO	2.8 ( <b>-0.61</b> )	2.3 (0.17)	1.8 ( <b>-0.52</b> )	2.3 ( <b>0.52</b> )
KAR	2.1 ( <b>-0.45</b> )	2.0 (0.14)	1.7 ( <b>-0.65</b> )	2.1 ( <b>0.46</b> )

Table 5.1: Average frequency [number of spells per year] of spells lasting 7 days or longer with trends [per decade] in parenthesis. **Bold values** are statistically significant (for a significance level  $\alpha = 0.05$ ).

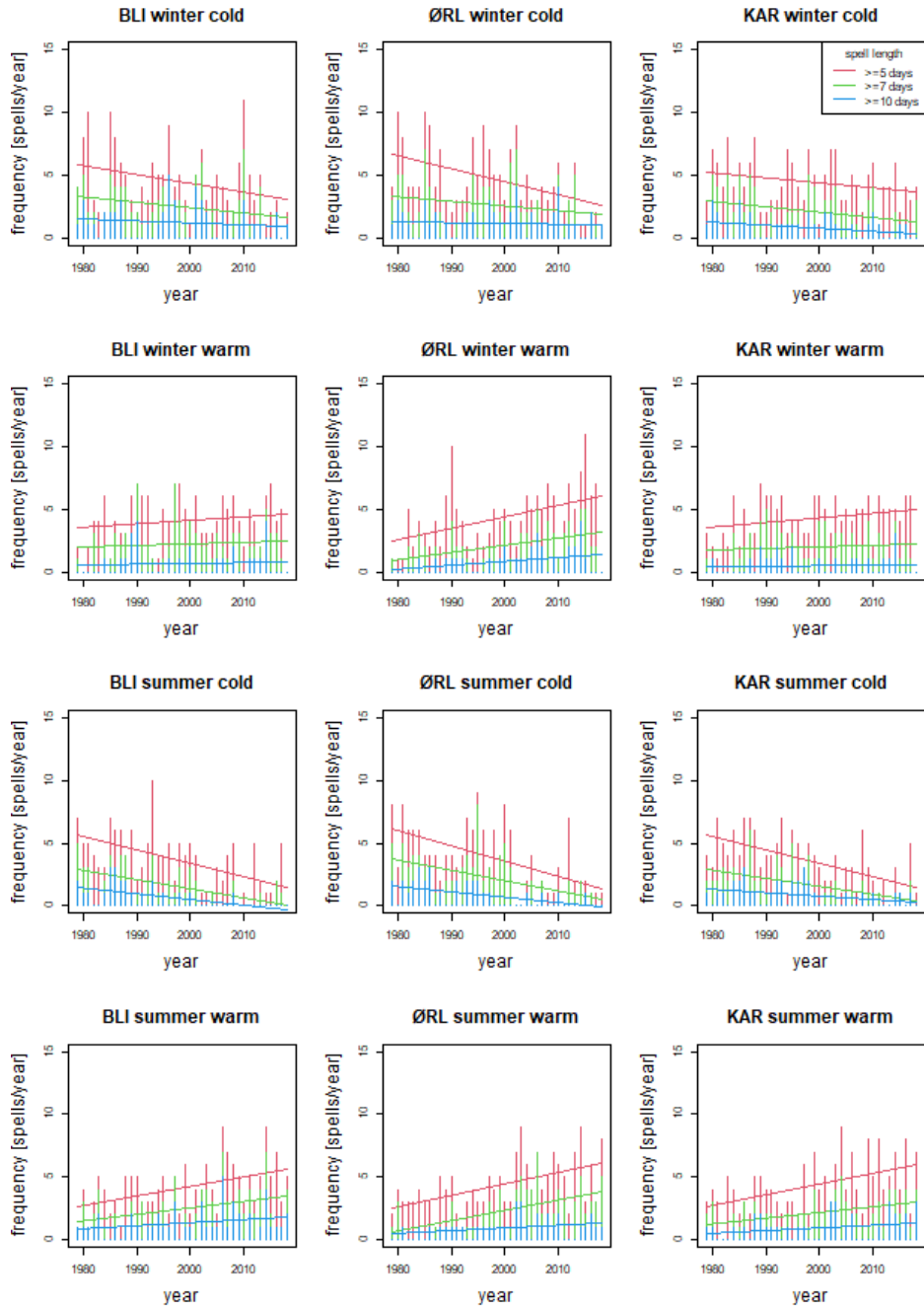


Figure 5.1: Frequency of cold and warm spells during winter and summer at three different locations. Vertical lines show number of spells for each year, while slanted lines show linear regression trends.

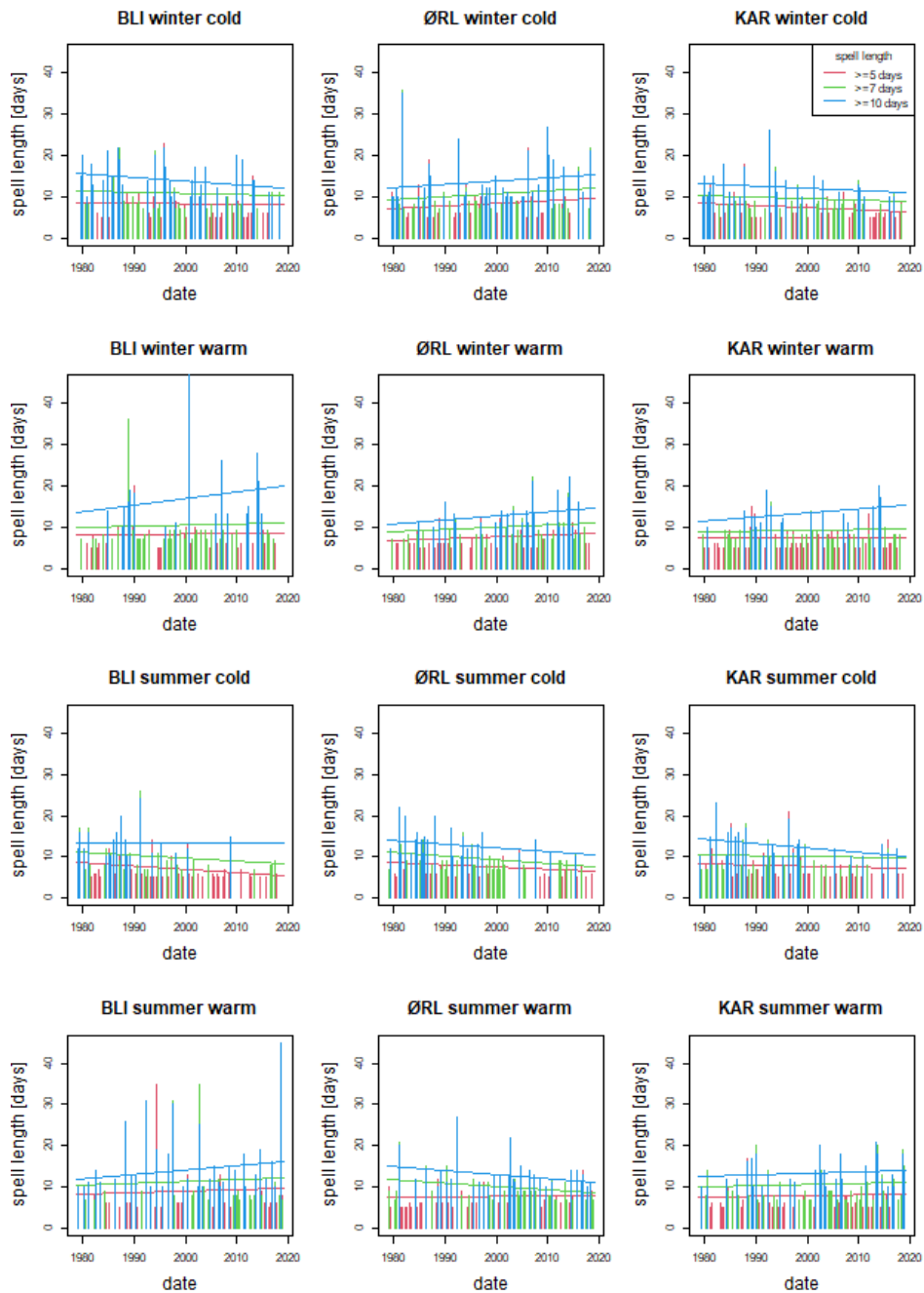


Figure 5.2: Length of cold and warm spells during winter and summer at three different locations. Vertical lines show length of every spell separately, while slanted lines show linear regression trends.

	winter, cold	winter, warm	summer, cold	summer, warm
BLI	10.9 (-0.25)	10.4 (0.31)	10.3 (-0.70)	11.4 (0.50)
TRY	11.2 (0.40)	10.8 (0.77)	9.3 (-0.48)	11.0 (0.29)
DRE	10.1 (0.49)	9.5 (-0.13)	9.0 ( <b>-0.51</b> )	10.8 (0.36)
BER	10.7 (-0.17)	10.1 (0.52)	9.6 ( <b>-0.86</b> )	10.6 (0.22)
ØRL	10.4 (0.70)	10.0 (0.55)	9.8 ( <b>-0.90</b> )	10.0 ( <b>-0.83</b> )
TRO	10.3 (-0.38)	9.5 (0.03)	9.9 (-0.53)	10.4 (0.21)
KAR	9.8 (-0.37)	9.3 (0.16)	10.3 (-0.16)	10.5 (0.27)

Table 5.2: Average length [days] of spells lasting 7 days or longer with trends [per decade] in parenthesis. **Bold values** are statistically significant (for a significance level  $\alpha = 0.05$ ).

Figure 5.2 shows length of every spell at three locations and trends calculated using linear regression. The other four locations are shown in the Appendix in Figure A.2. Again, notice that short spells ( $\geq 5$  days) can last longer than 10 days, but they do not necessarily overlap with long spells ( $\geq 10$  days). In addition, Table 5.2 shows average spell length with trend values for spells lasting 7 days or longer. Cold spells in summer are shortest almost everywhere, 1-2 days shorter than other types of spells. Trends are varying between locations within a single spell type and season, but also between different spell lengths. As an example, all locations have observed a slight increase in length of warm spells lasting 7 days or longer in summer, except ØRL, where the decrease has been greater than the increase at other locations. Outstanding trends are observed at ØRL, DRE and TRY for cold spells in winter which have got longer, as opposed to other locations where these spells got shorter. That happened despite the fact that cold spells got less frequent. Another outstanding trend is observed for warm spells in summer. While all other locations have experienced an increase in length of those spells, ØRL has experienced a decrease, even though the increase in frequency of warm spells in summer was largest just at ØRL.

## 5.2 Cold and warm spells and large-scale circulation relationship

Figure 5.3 shows 10 circulation types for Grosswettertypen classification (GWT10). For example, type 1 is high pressure in the south and low pressure in the north, resulting in strong westerly air transport in Norway, type 2 is high pressure in south and southeast and low pressure above Iceland, resulting in strong southwesterly flow, etc. Similar figures for other classification methods are shown in the Appendix (Figures A.3 - A.7).

What all these classification methods have in common is that all of them include at least one circulation type with strong low pressure system in the northern branches of the Atlantic Ocean transporting maritime air masses towards Norway, often referred to as NAO (as mentioned in Section 2.1). Another similarity is that all classification methods include at least



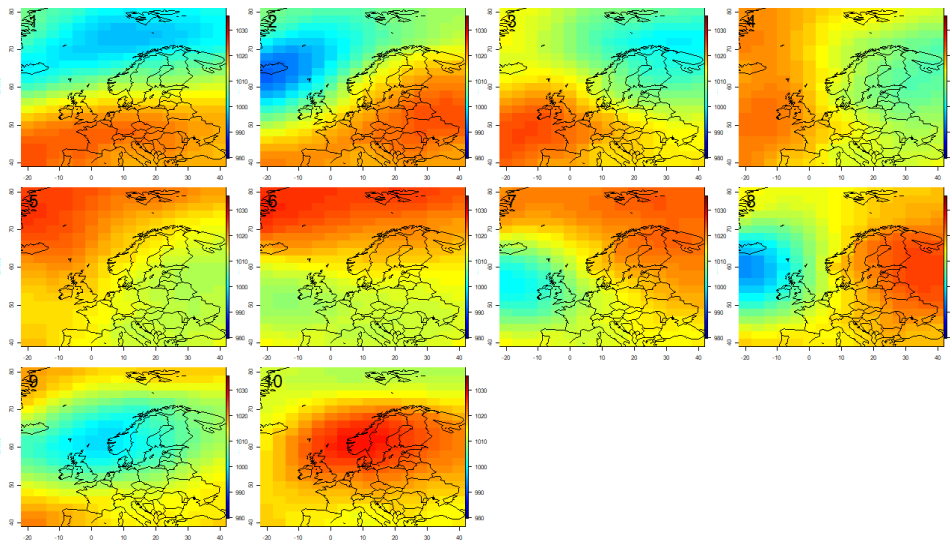


Figure 5.3: 10 circulation types for Grosswettertypen classification (GWT10). First axis indicates longitude, while second axis indicates latitude. Colors are showing sea level pressure (SLP) in hPa. Red: high SLP, blue: low SLP.

one circulation type with strong high pressure system above Scandinavia blocking the zonal air flow, a feature often called Scandinavian pattern, although the size and exact location of that high pressure system is varying between classification methods. In some cases the northern parts of Norway are still affected by the maritime air masses as the anticyclone is located above southern parts of Scandinavia.

Figure 5.4 shows the frequency of each circulation type using GWT10 during cold spells in winter for all locations, as well as changes in that frequency relative to the frequency during whole winter and the distribution of TAN for each circulation type. For BLI the most frequent CTs are 9 (cyclonic flow with centre outside of west coast of southern Norway), 10 (anticyclonic flow with centre above southern Norway), 6 (E flow) and 7 (SE flow). The least frequent CTs are 8 (S flow) and 5 (NE flow). Although 9 is the most frequent type during cold winter spells, the frequency is slightly lower than the seasonal frequency, while 5 being the second least frequent still has higher frequency than the seasonal. CTs with most positive frequency change are 6 and 10, but other CTs resulting in flow from easterly directions (5 and 7) as well as the one resulting in northerly flow (4) also have a positive change in frequency and are all considered to be associated with cold spells in winter (also see Table 5.3). CTs with strong atmospheric flow from westerly directions (1, 2, 3) are much less frequent. Additionally, the plot showing temperature ranges confirms that CTs with increased frequency are related to lowest TANs.

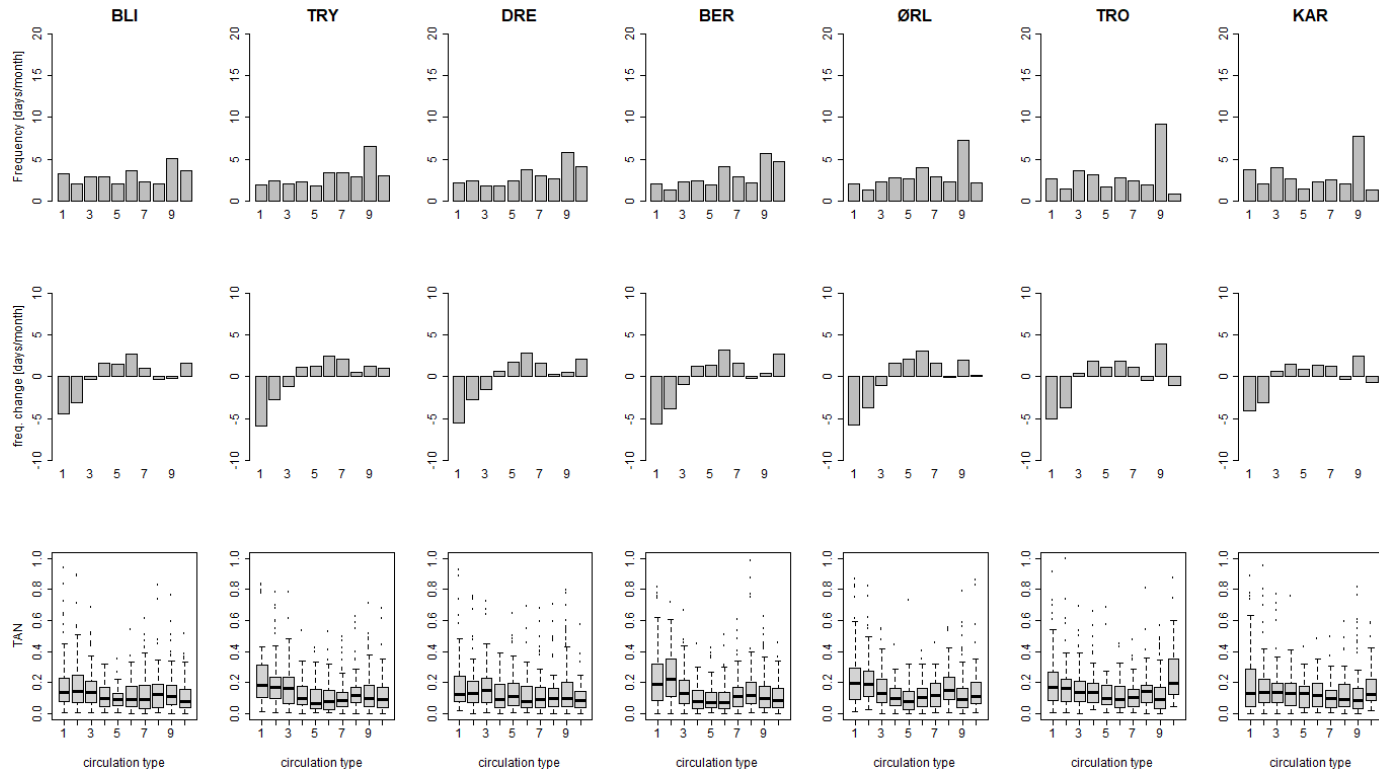


Figure 5.4: Circulation using GWT10 during cold spells in winter. **Top:** frequency of each circulation type [occurrence days/30 days]. **Middle:** change in frequency of each circulation type (frequency during cold spells in winter - frequency during winter) [occurrence days/30 days]. **Bottom:** TAN ranges of each circulation type as percentiles of TAN during winter.

CT number 9 appears to be the most frequent everywhere. The frequency of CT number 9 is especially high in the three northernmost locations (KAR, TRO, ØRL) which can be explained by air transport from land towards the sea. Furthermore, all locations are experiencing an increased frequency of CTs transporting continental and polar air masses towards Norway (4, 5, 6, 7), while there is a huge decrease in frequency of CTs transporting maritime air masses from the Atlantic Ocean (1, 2, 3).

Similar to Figure 5.4, Figure 5.5 shows the frequency of circulation types during warm spells in summer for all locations together with relative frequencies and TAX percentile ranges. In Southern Norway (BLI, TRY, DRE, BER), the most frequent type is type 10 (anticyclonic flow). Type 9 (cyclonic flow) is one of the least frequent in the south, but moving further north it becomes more frequent; at TRO it's frequency is more than twice of the second most frequent type. Types 1 and 3 (W and NW flow) are more frequent for Oslo (both BLI and TRY) than for other locations, especially the coastal ones (BER, ØRL, TRO), while types 6, 7 and 8 (E, SE and S flow) are more frequent for the same coastal locations, particularly for ØRL where type 7 is more frequent than any other type.

Many of the most frequent CTs also show the most positive change in frequency. Type 10 has positive relative frequency everywhere except at TRO. Types 7 and 8 also are more frequent than seasonal average everywhere, although the change is small for BLI and TRY and only slightly larger for DRE. Additionally, type 6 has positive relative frequency at all locations with exception of TRO and KAR. For type 2 the relative frequency is slightly negative only at the three southernmost locations (BLI, TRY, BER).

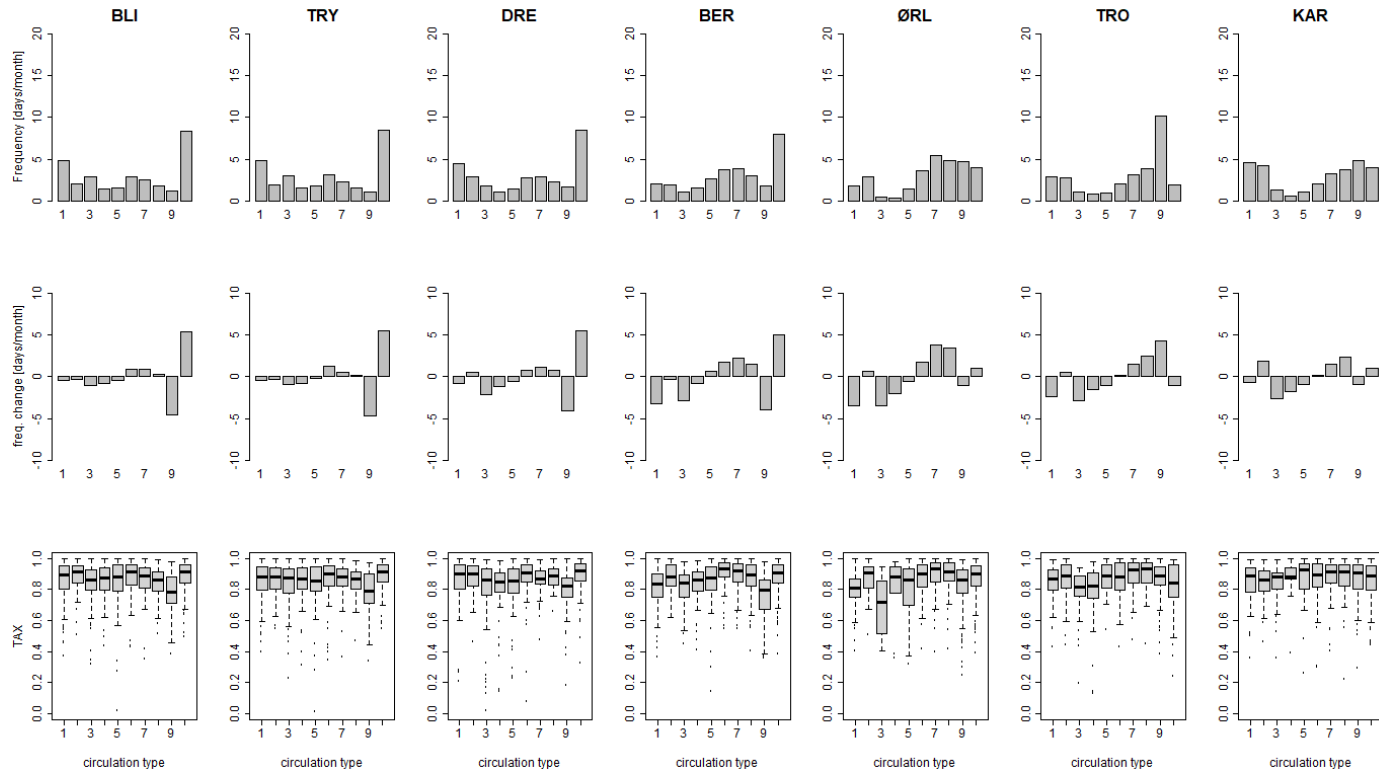


Figure 5.5: Circulation using GWT10 during warm spells in summer. **Top:** frequency of each circulation type [occurrence days/30 days]. **Middle:** change in frequency of each circulation type (frequency during cold spells in winter - frequency during winter) [occurrence days/30 days]. **Bottom:** TAN ranges of each circulation type as percentiles of TAN during winter.

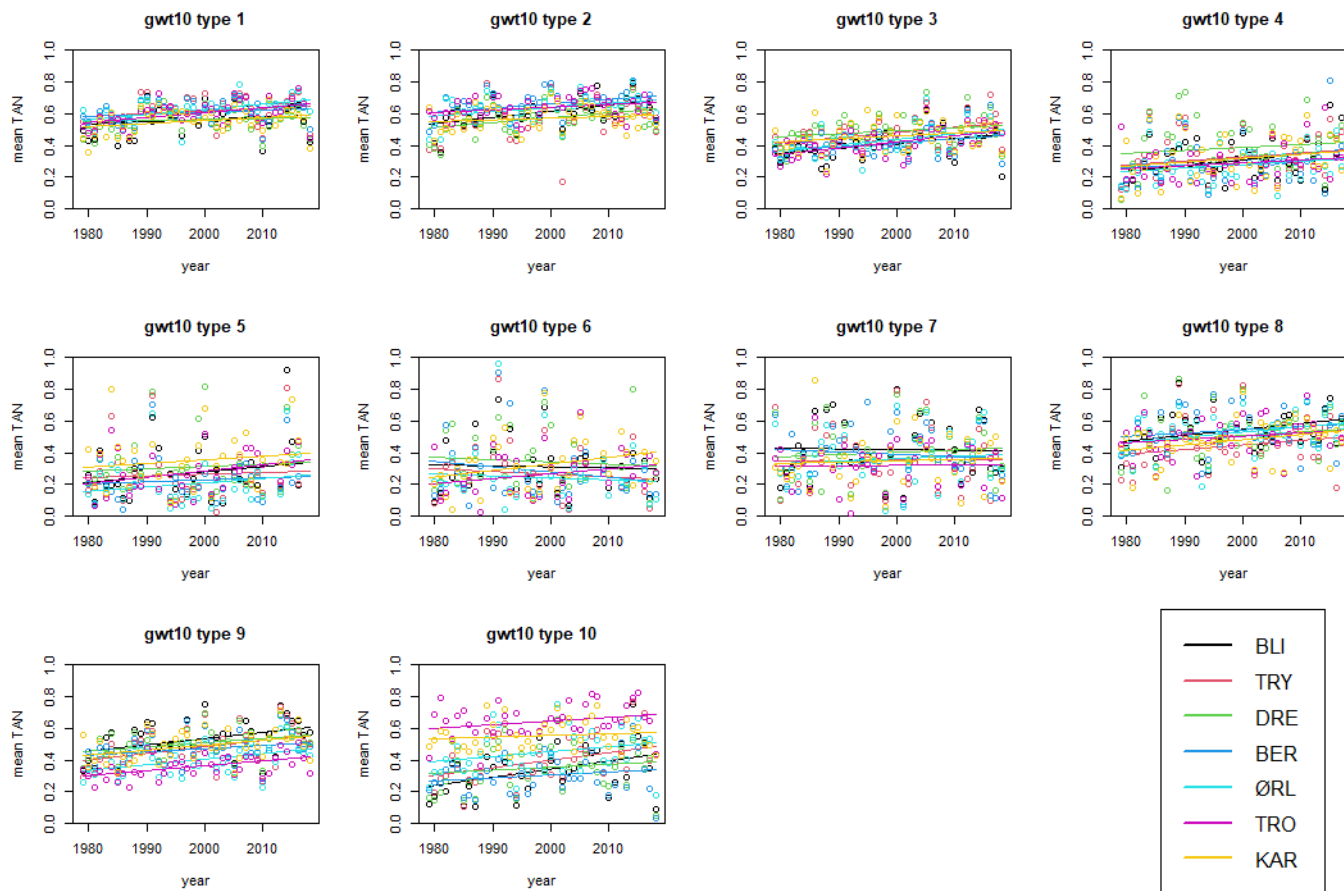


Figure 5.6: Mean T/AN in winter for all locations during different CTs for GWT10. Circles mark annual mean T/AN, while lines show trends.

Another approach to identify which circulation types are associated with cold and warm spells is to investigate mean minimum and maximum temperatures during different CTs at different locations for the entire season, as shown in Figure 5.6 for winter using GWT10 classification method. GWT10 types 1 and 2 (W and SW flow) are associated with rather high TAN everywhere, types 3, 7 (NW and SE flow) and 9 (a weak cyclone between Southern Norway and Faroe Islands) are resulting in TAN slightly below median, while for types 4, 5 and 6 (N, NE and E flow), TAN is rather low. TAN during type 10 (strong anticyclone above Scandinavia) is highly dependent on location: Northern Norway (TRO and KAR) is experiencing higher than average TAN, Central Norway (ØRL) is close to average, while in Southern Norway (BER, DRE, TRY and BLI) TAN is low. For almost all CTs all locations have experienced an increase in TAN, with exception of types 6 and 7. For type 7 (SE flow), although there are large interannual variations, there is no visible trend for any location. For type 6 (E flow), TAN in Northern Norway (TRO and KAR) has increased, while for other locations it has slightly decreased. In fact, while in the 1980s TAN in TRO and KAR was mostly lower than at other locations, the exact opposite was the case in the most recent decade.

Similar results are found for other classification methods: lowest TAN is associated with air flowing from N, NE and E, as well as strong high pressure systems (for places located close to or to the south of the centre) and small pressure gradients. On the other hand, highest TAN is associated with strong W and SW flow, usually coming from deep low pressure systems in the Norwegian Sea.

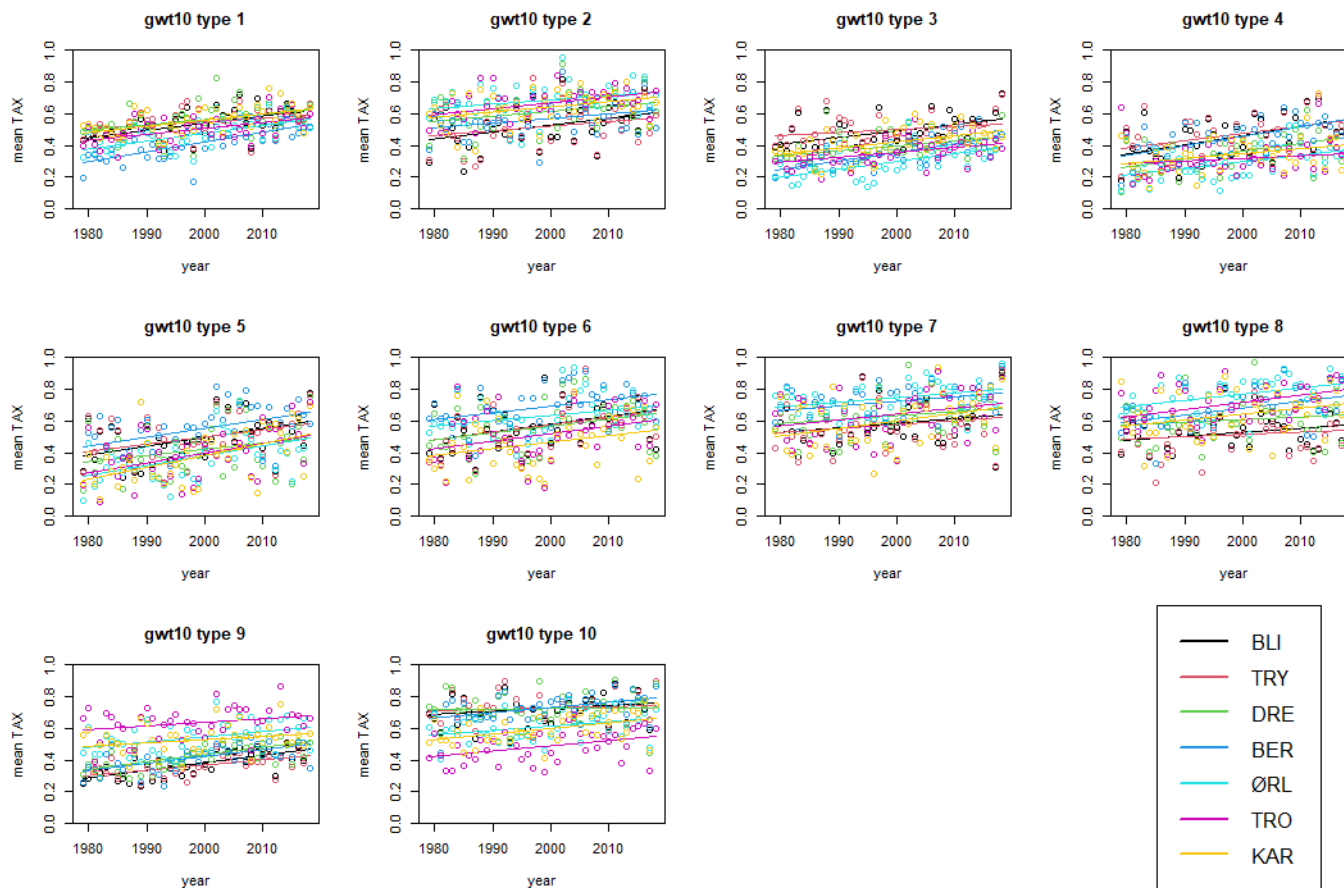


Figure 5.7: Mean TAX in summer for all locations during different CTs for GWT10. Circles mark annual mean TAX, while lines show trends.

Whereas extreme winter temperatures are highly depending on zonal direction of the air flow, summer extremes are rather depending on direction of the meridional flow, as shown in Figure 5.7. Again applying GWT10 classification method, the highest TAX is found for type 7 and 8 (SE and S flow). Types 2 and 6 (SW and E flow) are associated with TAX slightly above median, while types 1 and 5 (W and NE flow) has TAX close to or slightly below median. Types 3 and 4 (NW and N flow) are associated with rather low TAX. Type 9 and 10 (cyclonic and anticyclonic flow) are resulting in TAX almost opposite of each other; Southern Norway (BLI, TRY, DRE and BER) is experiencing low TAX in the case of type 9 and high TAX in the case of type 10, TAX in ØRL and KAR is close to median in both cases, while in TRO it is slightly higher than median for type 9 and slightly lower for type 10. TAX has been increasing everywhere for all CTs, although the rate is depending both on CT and location.

Once again, similar results are found for other classification methods: highest TAX is associated with air flowing from southerly directions, especially from S and SE, as well as for strong high pressure systems. For coastal locations (BER, ØRL and TRO), a combination of high pressure and S or SE air flow is particularly favorable for high TAX, whereas for inland locations in Southern Norway (BLI, TRY, DRE), high pressure systems with low air flow are favoring high TAX. Almost none of classification methods applied have any CTs associated with particularly high TAX in KAR, but southerly flow seems to be preferable.

Table 5.3 shows which CTs are associated with winter cold spells for each classification method and each location, meaning, as previously defined, that they are significantly more frequent during those spells than during the winter in general. As expected, CTs with transport of continental or arctic air masses towards Norway are associated with winter cold spells, though there are some regional differences such as GWT10 type 9 being present in all locations except BLI, DRE and BER. That could be explained by the weak low pressure system being centered right outside of the western coast of southern Norway, resulting in some relatively warm air transport from the sea south and southeast from that low pressure center. It is worth noticing that although this circulation type is not associated with winter cold spells at BLI, it is still associated with these at TRY. A possible explanation could be that temperature inversion is less frequent in this region for that CT, whereas lowest TANs in winter at BLI (as well as DRE and to some degree BER) are measured particularly during events of inverted vertical temperature profile. On the other hand GWT10 type 10 is not associated with winter cold spells in the three northernmost locations as opposed to the others further south, because of a strong high pressure system centered above southern Norway, so that the air moves from the sea towards the coast in Trøndelag and further north.



	GWT10	KMN09	LND09	PTT09	PXE10	SAN09
BLI	4, 5, 6, 7, 10	3, 4, 5, 8	3, 5, 8, 9	3, 4, 5, 7, 8, 9	2, 4, 6, 8	1, 5, 6, 7
TRY	4, 5, 6, 7, 9, 10	3, 4, 8	5, 8, 9	3, 4, 5, 6, 7, 8, 9	2, 3, 4, 6	1, 6, 7
DRE	4, 5, 6, 7, 10	3, 4, 6, 8	5, 8, 9	4, 5, 6, 7, 8, 9	2, 4, 6	1, 6, 7
BER	4, 5, 6, 7, 10	3, 4, 5, 8	3, 5, 8, 9	3, 4, 5, 6, 7, 8, 9	2, 4, 6, 8,	1, 5, 6, 7
ØRL	4, 5, 6, 7, 9	3, 4, 5, 8	3, 5, 8, 9	3, 4, 5, 6, 7, 8, 9	2, 4, 6	1, 5, 6
TRO	4, 5, 6, 7, 9	3, 4, 5,	3, 5, 6, 8	3, 4, 5, 7, 8, 9	2, 3, 5, 6	1, 5, 6, 8
KAR	4, 5, 6, 7, 9	3, 4, 5	3, 5, 6, 8	3, 4, 5, 8, 9	2, 3, 5, 6	1, 5, 6, 8

Table 5.3: CTs associated with cold spells during winter based on their relative frequency.

	GWT10	KMN09	LND09	PTT09	PXE10	SAN09
BLI	6, 7, 10	7, 8	4, 7, 9	2, 4, 5, 6	1, 2, 4, 8	4, 5, 6, 7
TRY	6, 7, 10	7, 8	4, 7, 9	2, 4, 5, 7	1, 2, 4, 8	4, 5, 6, 7
DRE	6, 7, 8, 10	6, 7, 8	4, 9	2, 4, 5, 6	1, 2, 4	4, 6, 7
BER	5, 6, 7, 8, 10	7, 8	4, 5, 9	2, 4, 5, 6, 7	1, 2, 4	6, 7
ØRL	2, 6, 7, 8, 10	4, 8	2, 5, 9	5, 6, 7	2, 3, 4, 10	6, 7, 9
TRO	7, 8, 9	4, 8, 9	2, 5, 6, 9	1, 5	3, 9, 10	1, 6, 7, 9
KAR	2, 7, 8, 10	6, 8, 9	2, 4, 9	1, 2, 5	1, 2, 3, 10	7, 9

Table 5.4: CTs associated with warm spells during summer based on their relative frequency.

	winter, cold	winter, warm	summer, cold	summer, warm
BLI	2.5 (-0.03)	2.7 (0.06)	2.0 (-0.08)	3.1 (-0.05)
TRY	2.5 (-0.05)	3.0 (0.05)	2.6 (-0.11)	3.0 (-0.05)
DRE	2.0 (0.02)	3.4 (0.11)	2.8 (-0.05)	2.6 (0.02)
BER	2.5 (-0.05)	3.7 (0.12)	2.6 (-0.17)	2.5 (0.09)
ØRL	2.5 (-0.07)	4.3 (0.06)	2.4 (-0.13)	2.5 (0.08)
TRO	2.5 (-0.08)	2.3 (-0.08)	2.7 (-0.04)	3.0 (0.08)
KAR	2.4 (-0.09)	3.1 (0.05)	1.8 (-0.04)	2.7 (0.03)

Table 5.5: Average frequency [number of spells per year] of periods of persistent circulation lasting 7 days or longer with trends [per decade] in parenthesis as an average of all six classification methods.

Using the information from, inter alia, Figure 5.4 and Table 5.3 one can find periods of persistent circulation and identify temperatures at each location during those periods to see whether CTs which are assumed to be associated with cold and warm spells actually can be used to find cold and warm spells. Figure 5.8 shows how, on average, the temperature evolves for each day of these periods of persistent circulation using different classification methods. In most cases the temperature on first day is close to the median temperature, but as time goes, the temperature is decreasing in case of cold spells and increasing in case of warm spells. In many cases, around the fourth day, the temperature approaches a sort of equilibrium when there is no much further change in temperature later on. In some cases there are some large "jumps" from around day 10, which can be explained by a low number of events of persistent circulation exceeding that length and thus resulting in too few data points to obtain the true mean.

### 5.3 Large-scale circulation trends

Figure 5.9 (and Figure A.9) together with Table 5.6 show frequency of periods of persistent circulation associated with cold and warm spells as an average of all six classification methods. It appears that periods of persistent circulation associated with warm spells in winter are most frequent almost everywhere, especially at BER and ØRL. Although trends do not show any large changes in frequency, there are still some similarities between locations. Frequency of periods of persistent circulation associated with cold spells both in winter and summer is mostly decreasing, whereas for those associated warm spells it is mostly increasing. As for the length of such periods, Table 5.6 shows that periods of persistent circulation associated with cold spells in summer are shortest and still getting shorter everywhere. For cold spells in winter the length is increasing for every location, with largest increase at coastal locations in Southern Norway (BER and ØRL) and smallest increase in Northern Norway (TRO and KAR). On the other hand, periods associated with warm spells in summer are getting shorter along the coast (BER, ØRL and TRO) and longer at inland locations.

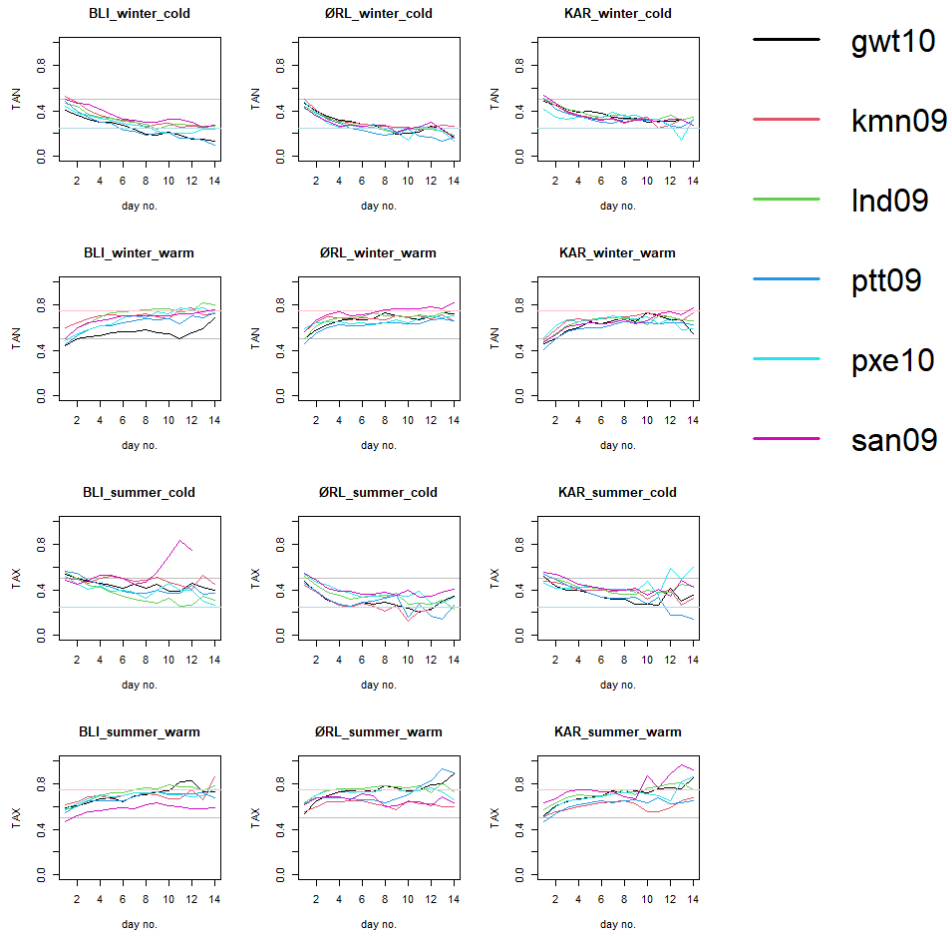


Figure 5.8: Average temperature on each day of periods of persistent circulation based on CTs associated with each kind of spell. Horizontal lines are corresponding to the median temperature (gray), 25th percentile (light blue) and 75th percentile (light red).

	winter, cold	winter, warm	summer, cold	summer, warm
BLI	11.2 (0.22)	10.5 (0.10)	9.2 (-0.15)	10.6 (0.06)
TRY	10.9 (0.13)	10.8 (0.06)	10.0 (-0.23)	10.5 (0.10)
DRE	10.9 (0.12)	11.0 (-0.02)	9.8 (-0.20)	10.0 (0.07)
BER	11.2 (0.29)	11.3 (-0.06)	9.6 (-0.01)	10.1 (-0.04)
ØRL	10.8 (0.33)	11.5 (-0.03)	9.3 (-0.07)	10.0 (-0.22)
TRO	10.4 (0.10)	10.0 (0.22)	9.7 (-0.11)	10.3 (-0.43)
KAR	10.2 (0.06)	10.5 (-0.12)	9.6 (-0.17)	10.2 (0.25)

Table 5.6: Average length [days] of periods of persistent circulation lasting 7 days or longer with trends [per decade] in parenthesis as an average of all six classification methods.

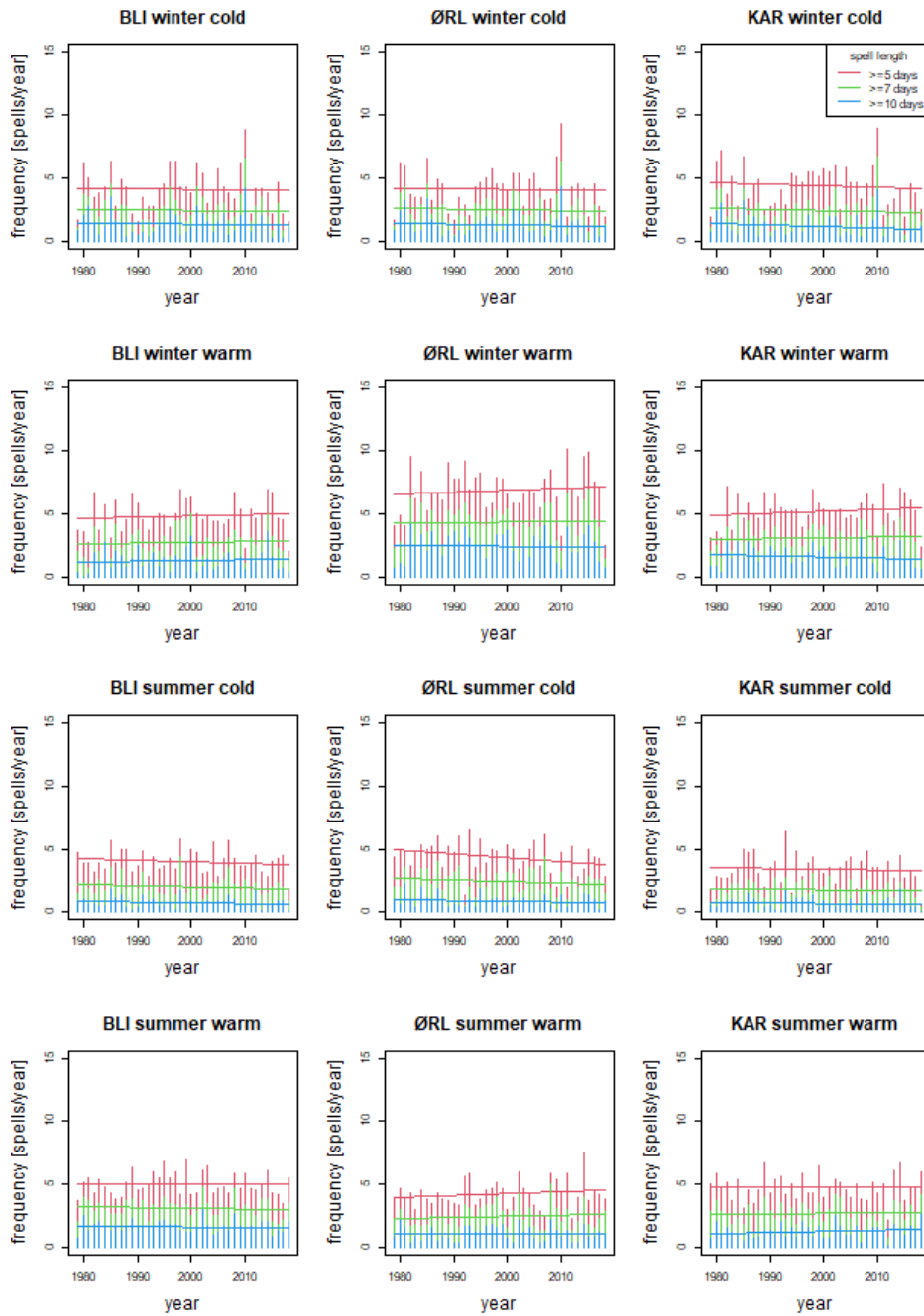


Figure 5.9: Frequency of periods of persistent circulation resulting in cold and warm spells during winter and summer in three different locations as an average of all six classification methods. Vertical lines show number of periods for each year, while slanted lines show linear regression trends.

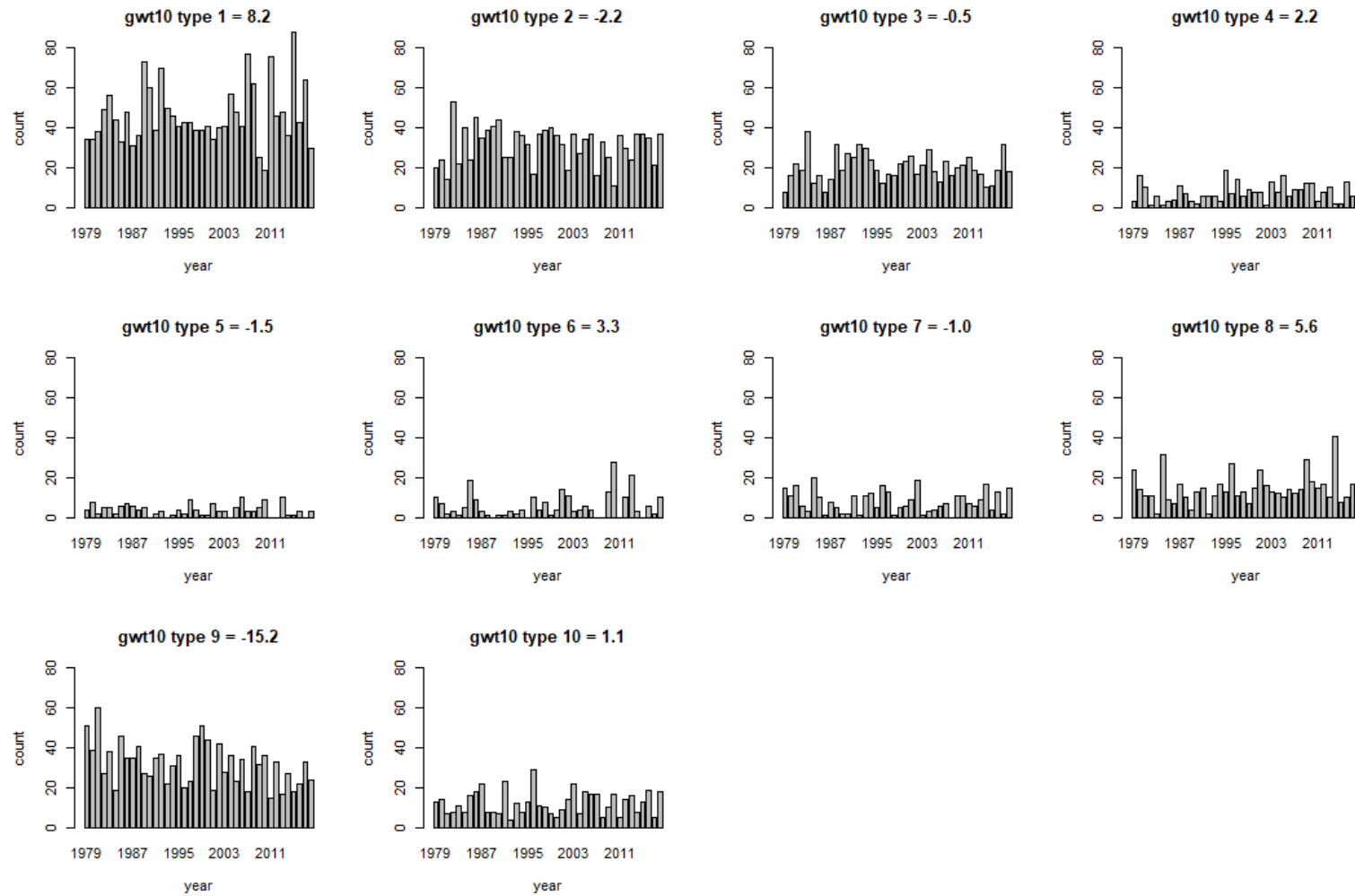


Figure 5.10: Annual number of days of different CTs occurring during winter for GWT10. Values above each plot show change in average number of days per year from 1979 to 2018.

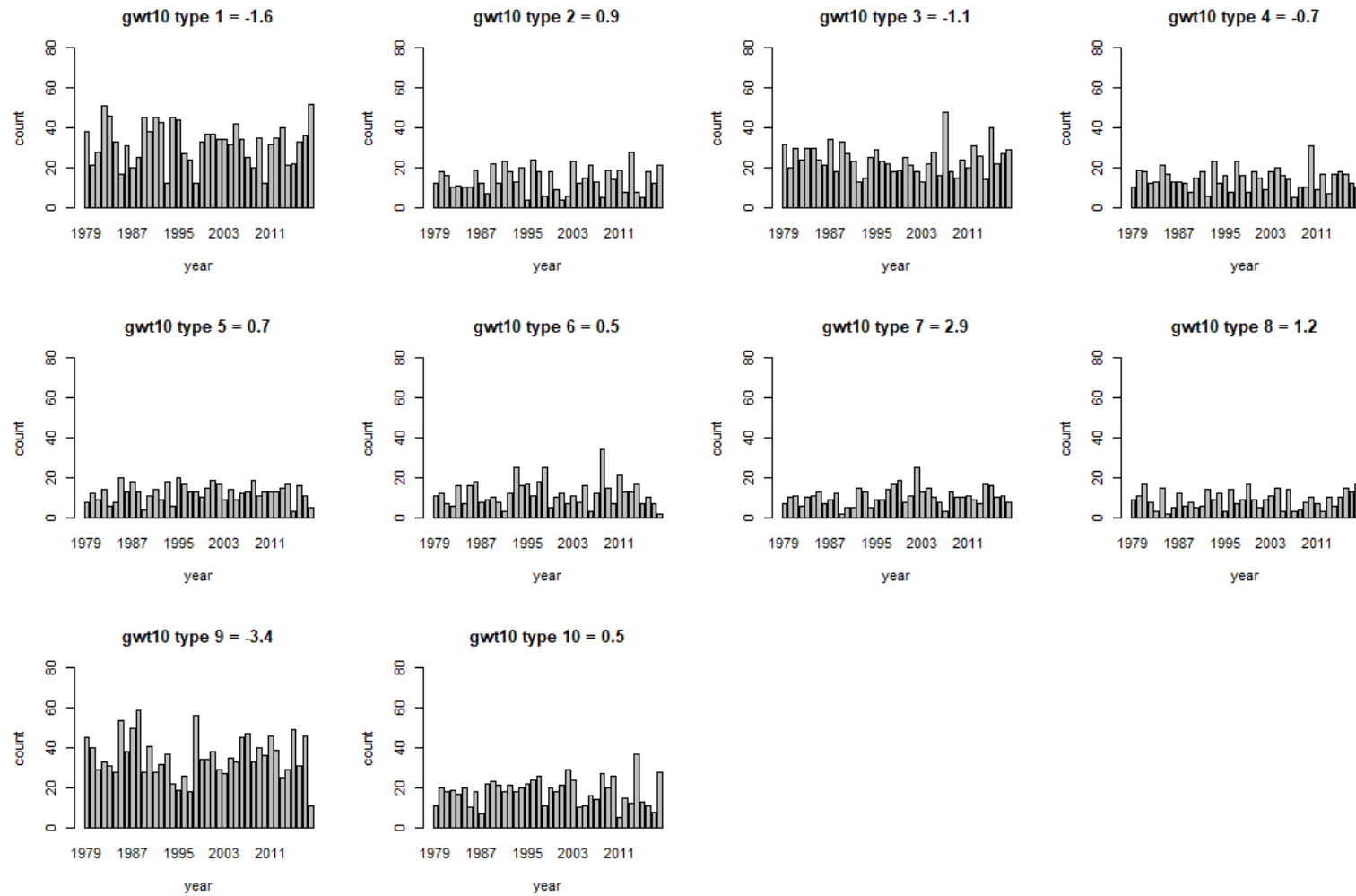


Figure 5.11: Annual number of days of different CTs occurring during summer for GWT10. Values above each plot show change in average number of days per year from 1979 to 2018.

To determine whether there has been any change in atmospheric circulation leading to persistent cold and warm spells, it is also possible to examine frequency of each circulation type during the season of interest in general, such as shown in Figures 5.10 and 5.11 for winter and summer respectively. For winter circulation, GWT10 type 1 (W flow) is overall the most frequent, followed by types 2, 3 and 9 (SW, NW and cyclonic flow). Flow from easterly directions (types 5, 6 and 7) as well as directly from north (type 4) is much less frequent, rarely exceeding two weeks per year for each of those CTs and some years being completely absent. As for trends, the greatest change is found for type 9 (weak cyclonic flow) with an average loss of 15 days per year from 1979 to 2018. Other CTs with a noticeable decrease in frequency are types 2, 5 and 7 (SW, NE and SE flow). On the opposite side with increased frequency are types 1, 4, 6, 8 and 10 (W, N, E, S and anticyclonic flow).

Examining other classification methods yields somewhat similar results: an increasing frequency of deep low pressure systems in the Norwegian and Barents Seas, while number of weak cyclones located close to Southern Norway is decreasing. Regarding Scandinavian highs, different classification methods show different trends depending on the exact placement of the anticyclone.

As shown in Figure 5.11, atmospheric circulation during summer differs from the winter circulation. Even though types 1, 3 and 9 (W, NW and cyclonic flow) are still dominating, their frequency is much closer to the least frequent types. Number of days with these three types has also decreased, while frequency of types 7 and 8 (SE and S flow) has increased. Frequency of other CTs is mostly unchanged.

Comparing all classification methods, high pressure systems located above Scandinavian Peninsula/Gulf of Bothnia seem to be occurring more frequently, while low pressure systems above Barents Sea/Kola Peninsula are less frequent.



## Chapter 6

# Discussion

The results presented in Chapter 5 show that during the 1979-2018 period there has been a change in frequency of both cold and warm spells in winter as well as in summer; furthermore there has been a change in atmospheric circulation and temperature associated with different circulation types. The question arises: could change in the atmospheric circulation explain the change in frequency of cold and warm spells?

First of all, which circulation types are generally associated with high and low temperatures in Norway, disregarding regional differences, and how has their frequency changed? As shown in Table 5.3, some CTs associated with cold spells in winter are appearing for all locations, such as types 4, 5, 6, 7 and 9 for GWT10, types 3, 4 and 8 for KMN09 or types 1, 5 and 6 for SAN09. These are also confirmed as being connected to cold weather by examining average TAN during each CT for winter in general. What they all have in common is a weak air flow, preferably of continental and/or Arctic origin. On the other hand there are some CTs leading to TAN being higher than seasonal average, such as types 1 and 2 for GWT10, types 1, 2 and 9 for KMN09 and types 2, 3, 4 and 9 for SAN09; it is less likely that a cold spell will persist during these CTs. A common feature for those CTs is a deep low pressure system in or close to the Norwegian Sea. By analysing trends for every CT, the CTs associated with cold spells became, summed up, less frequent, whereas CTs associated with TAN being higher than average became more frequent, as shown in Figure 6.1. With a decreasing number of days with "cold" CTs and an increasing number of days with "warm" CTs, it should be expected that cold spells would be less frequent.

Further on, an analysis of the frequency of periods of persistent circulation associated with cold and warm spells in winter shows that periods of "cold" circulation lasting for several days are getting slightly less frequent, while periods of "warm" circulation are generally more frequent, although the rate of change is much smaller than for actual cold and warm spells. As shown in Figure 5.6, TAN has been increasing during the 1979-2018 period at all locations for almost every CT, which would contribute to the rapid change in frequency of cold and warm spells in winter.

As for warm spells during summer season, associated CTs for Norway in general appear to be types 6, 7, 8 and 10 for GWT10, types 4, 5 and 9

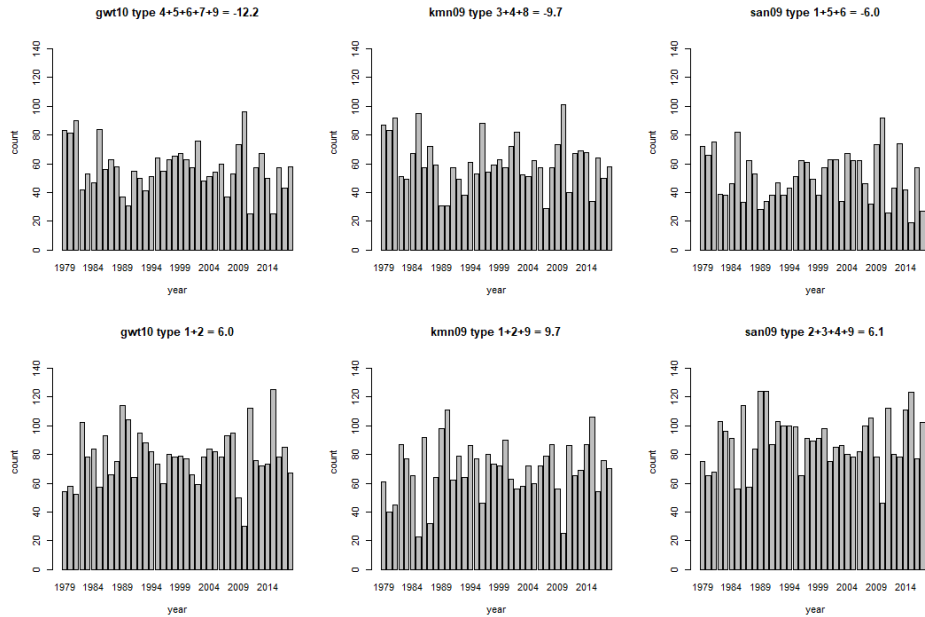


Figure 6.1: Annual number of days of all CTs associated with cold (top panel) and warm (bottom panel) spells during winter for three classification methods. Values above each plot show change in average number of days per year from 1979 to 2018.

for LND09 or types 2, 5 and 6 for PTT09. A common feature for those CTs is weak flow of continental and/or subtropical air masses, preferably with high pressure systems covering Norway. Some CTs resulting in low TAX are types 1, 3, 4 and 9 for GWT10, types 3, 7 and 8 for LND09 or types 1 and 3 for PTT09. All of those are featuring flow of arctic air masses towards Norway. Once again, analysing frequency of these sets of CTs as shown in Figure 6.2 indicates that CTs favoring high TAX have become more frequent, while CTs resulting in low TAX got less frequent. Just like for winter, with an increasing number of "warm" CTs together with a decreasing number of "cold" CTs, combined with an overall increase in TAX for all CTs, a higher number of warm spells should be expected.

Looking at some regional differences, number of warm spells in summer is increasing fastest at BER and ØRL. These locations, being situated along the coast, are experiencing highest TAX when land breeze is dominating throughout the day. That condition is satisfied during air flowing from east, southeast and south, such as types 6, 7 and 8 for GWT10, as opposed to other locations where highest TAX occurs either under the regime of high pressure systems (GWT10 type 10 for BLI, TRY and DRE) or for other general directions of air flow (GWT10 type 9 for TRO, type 2 for KAR). These three CTs, on average being the least frequent, are occurring more often in the course of years in contrast to types 2, 9 and 10 being more frequent on average and either decreasing in frequency or increasing at a lower rate than sum of types 6, 7 and 8.

Additionally, as shown in the previous chapter, ØRL has some

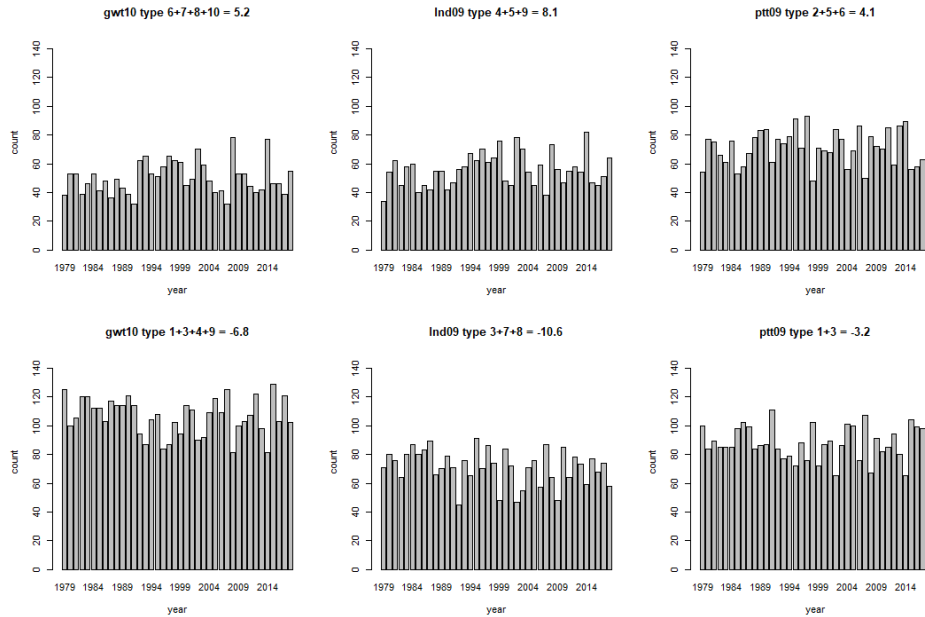


Figure 6.2: Annual number of days of all CTs associated with cold (top panel) and warm (bottom panel) spells during summer for three classification methods. Values above each plot show change in average number of days per year from 1979 to 2018.

outstanding trends in frequency and length of warm spells in summer. Whereas the frequency is increasing at a higher rate than at any other location, the trend for length of these spells is negative as opposed to other locations. One possibility is that in the early years, the few warm spells were solely due to unusually long but infrequent periods of persistent circulation associated with high TAX, whereas in the later years there has been an increasing number of short spells not only due to change in the atmospheric circulation, but also due to an increase in TAX associated with each circulation type. In other words, four decades ago high TAX could be measured mostly during certain CTs, while most recently high TAX has also been measured during CTs not typically associated with warm air increasing length of short spells when the circulation patterns are changing quickly.

To conclude, in the most recent years Norway in general has experienced more frequent warm spells both in summer and winter, but also less frequent cold spells in both seasons. At the same time there has been a change in the atmospheric circulation above Europe and northern branches of the Atlantic Ocean with more frequent strong cyclones in the Norwegian Sea and less frequent transport of continental air masses towards Norway in winter, while in summer high pressure systems above Scandinavia and Gulf of Bothnia are present more often, whereas the opposite is true for low pressure systems in the Barents Sea/Kola Peninsula region. These changes in the atmospheric circulation are expected to result in the observed trends in the frequency of cold and warm spells, although they alone do not ex-

plain the magnitude of trends. Nevertheless, some local differences are possibly connected to these changes.

## Chapter 7

# Summary and outlook

The aim of this analysis was to investigate whether different regions in Norway, represented by selected locations, have experienced changed frequency and/or persistence of cold (TAN below the 25th percentile) and warm (TAX above the 75th percentile) spells in the most recent decades and whether these changes could be explained by changes in the atmospheric circulation in Europe. To find trends in frequency and length of spells, measurements from the Norwegian Meteorological Institute's stations were analyzed. Later on, cost733class software was applied to atmospheric sea level pressure from the global reanalysis ERA5 in order to analyze atmospheric circulation patterns in Europe using different classification methods.

The results indicate that both the frequency and the persistence of spells of interest indeed are changing in time with some long-term trends, although the trends are varying both between locations and seasons. All locations have experienced a decreasing number of cold spells of all lengths both during winter and summer, and an increasing number of warm spells of all lengths both during winter and summer, although the frequency of short spells ( $\geq 5$  days) is changing at a higher rate than the frequency of long spells ( $\geq 10$  days). The results for spell length show that, in general, during summer warm spells have got longer, while cold spells have got shorter. Similar to summer, warm spells in winter are generally longer than a few decades ago.

The analysis of the relationship between spells of interest and the atmospheric circulation has shown that the direction of the atmospheric flow has strong impact on the temperature, although the temperature anomaly for a single circulation type is seasonally dependent. For winter, cold spells can be expected in regions where the horizontal pressure gradient is small and/or during flow of continental air masses of arctic origin (E and NE flow), whereas warm spells are associated with strong flow from west and southwest. For summer, continental air masses of subtropical origin (SE and S flow) are resulting in warm spells, particularly along the western part of the Norwegian coast where that flow is dominating over the sea breeze due to temperature contrasts between sea and land during the day, while for inland locations in Southern

Norway high pressure systems with negligible air flow lead to highest temperatures. In contrast, air flowing from the high Arctic (NW, N and partly NE) is associated with cold spells.

As for the evolution of the atmospheric circulation during past four decades, there are some indications of an increase in frequency of days with deep low pressure systems in the Norwegian and Barents seas during winter as well as a decreasing frequency of days with continental air flow. During summer, number of days with low pressure system in the region of Kola Peninsula resulting in N flow has got lower, while days with Scandinavian pattern are more frequent. Combining circulation types associated with warm and cold spells specific for each location gives an indication of general trends being slightly increasing for CTs associated with warm spells and slightly decreasing for CTs associated with cold spells, both for winter and summer.

Even though the trends for atmospheric circulation associated with cold and warm spells mostly show the same direction as actual frequency of cold and warm spells, the magnitudes are much larger for measured spells. A possible explanation is that the temperature measured during each circulation type has been gradually increasing in most cases, increasing the probability of the occurrence of warm spells and decreasing it for cold spells. The length of warm spells has been decreasing for cold spells in summer and mostly increasing for both seasons with a few exceptions. At ØRL, where warm spells in summer have increased in frequency but decreased in length, a possible reason is that few extremely long but infrequent resulted in a high average length in the beginning of the analyzed time period, whereas later on as the average temperature has been increasing, the frequency of shorter spells has been increasing resulting in a lowering of the average length. The reason why it has not been observed at other locations could be the characteristics of the local climate with smaller differences between average and extreme temperatures due to large influence from the sea.

Overall, the changes in the atmospheric circulation are possible to account for a part of change the frequency of cold and warm spells in Norway, but a dominating factor is, nevertheless, an increasing temperature for all circulation types.

For a further study it would be recommended to apply the same classification methods on pressure at different altitudes, e.g. geopotential height at 500 hPa, in order to see if there is a stronger connection to cold and warm spells, or even add more classification methods to look at average trends. As northern parts of Norway, in particular Karasjok, are close to the outer borders of the domain used for classification of the circulation types, the domain could be expanded towards east to see if a better relation between circulation types and temperature extremes in that region could be achieved. A possible uncertainty was also due to comparing of daily minimum/maximum temperature to daily-mean pressure field. Comparing of temperature measurements to the pressure field at the exact same moment could provide a better connection between temperature and circulation types.

# Bibliography

- [1] Anthony G. Barnston and Robert E. Livezey. 'Classification, Seasonality and Persistence of Low-Frequency Atmospheric Circulation Patterns'. In: *Monthly Weather Review* 115.6 (June 1987), pp. 1083–1126. ISSN: 0027-0644. DOI: 10.1175/1520-0493(1987)115<1083:CSAPOL>2.0.CO;2.
- [2] Hans Hersbach et al. 'The ERA5 global reanalysis'. In: *Quarterly Journal of the Royal Meteorological Society* 146.730 (2020), pp. 1999–2049. DOI: <https://doi.org/10.1002/qj.3803>. eprint: <https://rmets.onlinelibrary.wiley.com/doi/pdf/10.1002/qj.3803>. URL: <https://rmets.onlinelibrary.wiley.com/doi/abs/10.1002/qj.3803>.
- [3] Radan Huth et al. 'Classifications of Atmospheric Circulation Patterns - Recent Advances and Applications'. In: *Trends and Directions in Climate Research: Ann. N.Y. Acad. Sci.* 1146: 105–152 (2008).
- [4] H.H. Lamb. 'British Isles Weather types and a register of daily sequence of circulation patterns, 1861-1971.' In: *Geophysical Memoir* 116 (1972), 85pp.
- [5] Andreas Philipp et al. *cost733class-1.2 User Guide*. 2014. URL: <http://cost733.geo.uni-augsburg.de/cost733class-1.2>.
- [6] Andreas Philipp et al. 'Development and comparison of circulation type classifications using the COST 733 dataset and software'. In: *INTERNATIONAL JOURNAL OF CLIMATOLOGY* (2014).
- [7] Ole Einar Tveito et al. *COST Action 733: Harmonization and Application of Weather Type Classifications for European Regions - Final scientific report*. 2016, 422pp. URL: [https://opus.bibliothek.uni-augsburg.de/opus4/frontdoor/deliver/index/docId/3768/file/COST733\\_final\\_scientific\\_report\\_2016.pdf](https://opus.bibliothek.uni-augsburg.de/opus4/frontdoor/deliver/index/docId/3768/file/COST733_final_scientific_report_2016.pdf).
- [8] Peter C. Werner and Friedrich-Wilhelm Gestengarbe. 'Katalog der Grosswetterlage Europas (1881-2009) nach Paul Hess und Helmut Brezowsky 7., verbesserte und ergänzte auflage'. In: *PIK Report* (2010). ISSN: 1436-0179.

**Appendix A**

**Appendix**



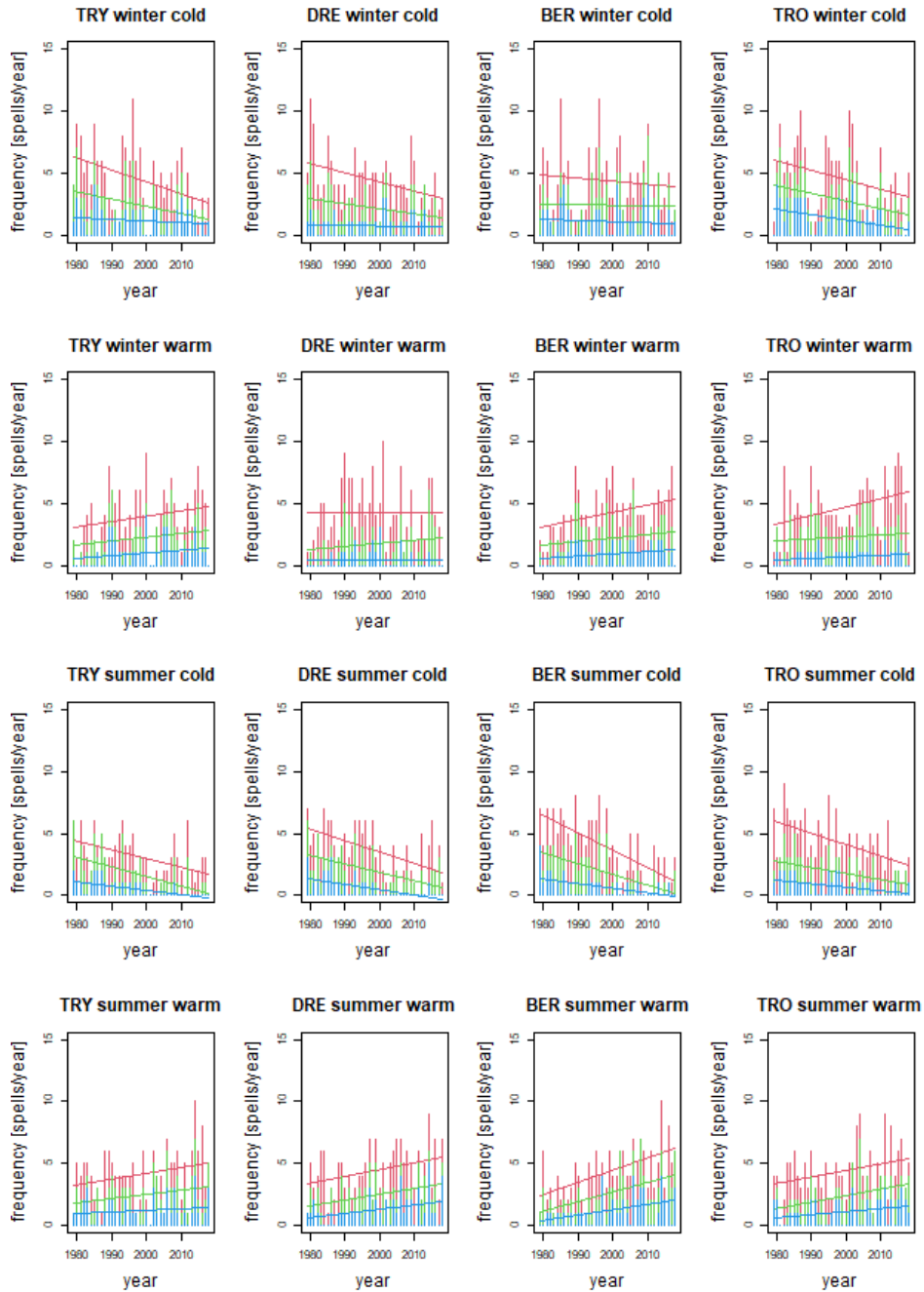


Figure A.1: Frequency of cold and warm spells during winter and summer in four different locations. Vertical lines show number of spells for each year, while slanted lines show linear regression trends.

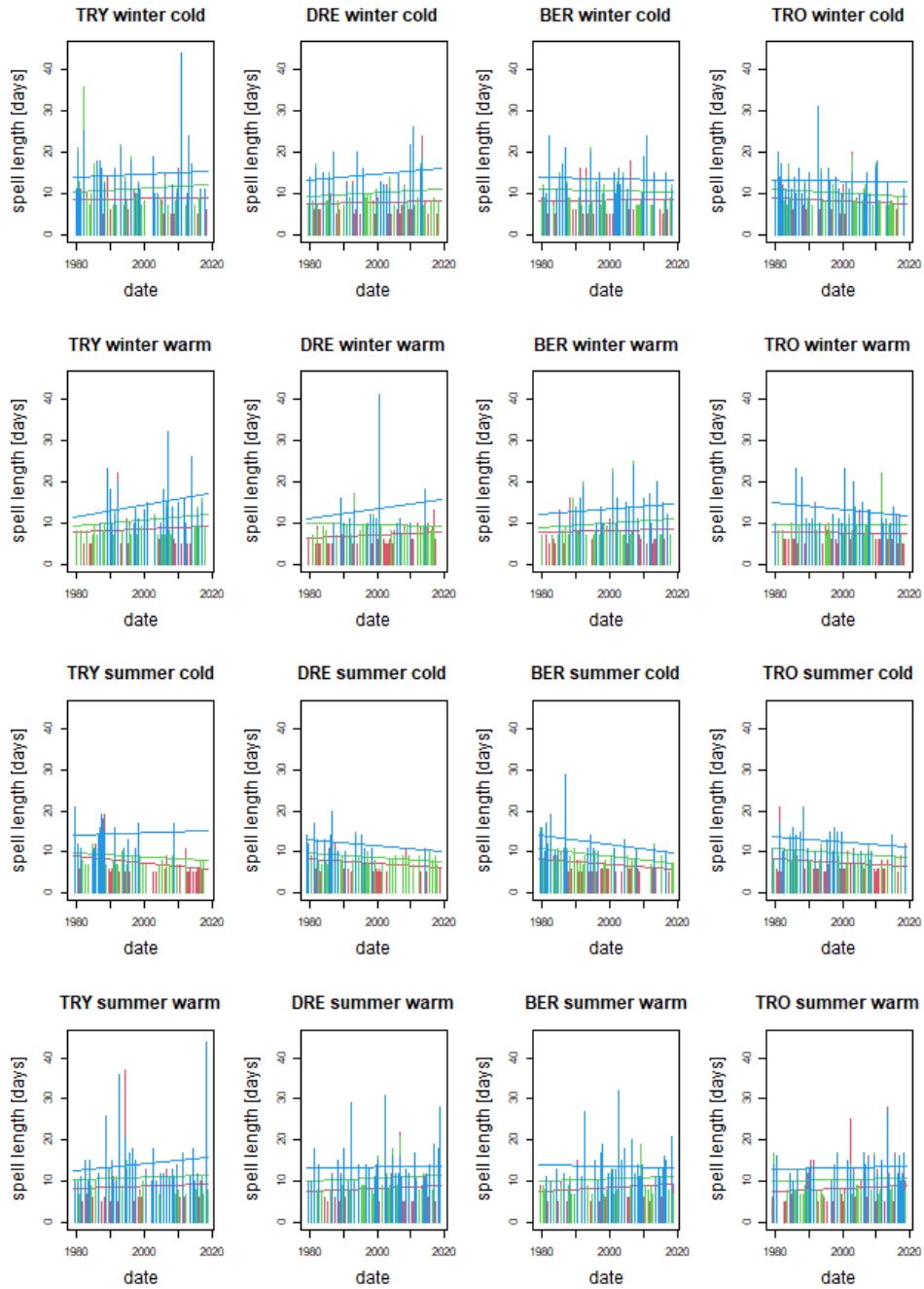


Figure A.2: Length of cold and warm spells during winter and summer in four different locations. Vertical lines show length of every spell separately, while slanted lines show linear regression trends.

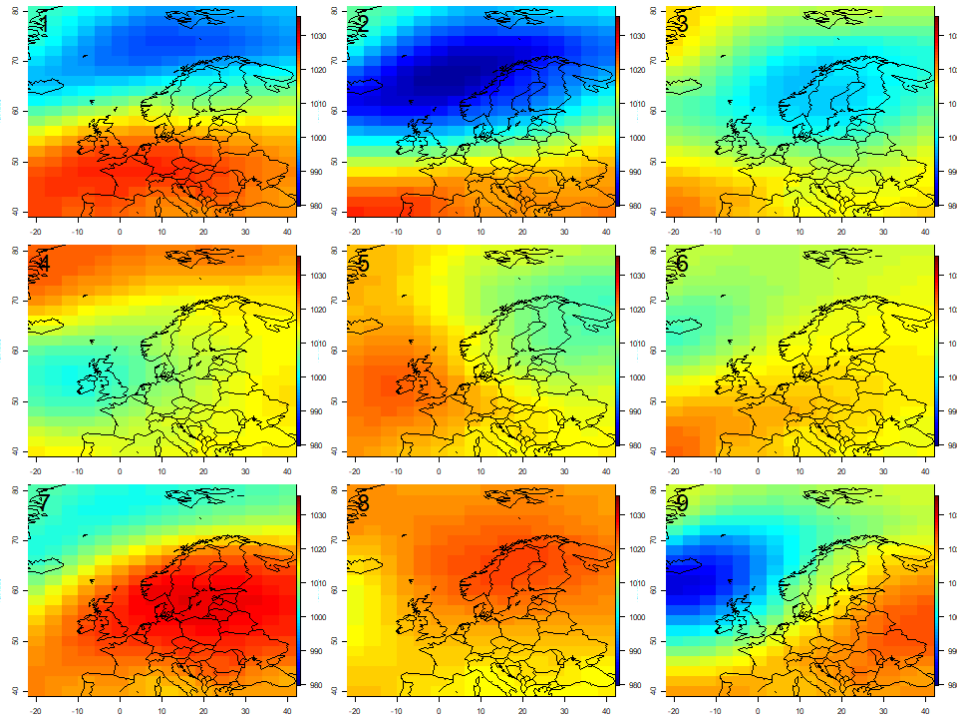


Figure A.3: 9 circulation types for k-means classification (KMN09). First axis indicates longitude, while second axis indicates latitude. Colors are showing sea level pressure (SLP) in hPa. Red: high SLP, blue: low SLP.

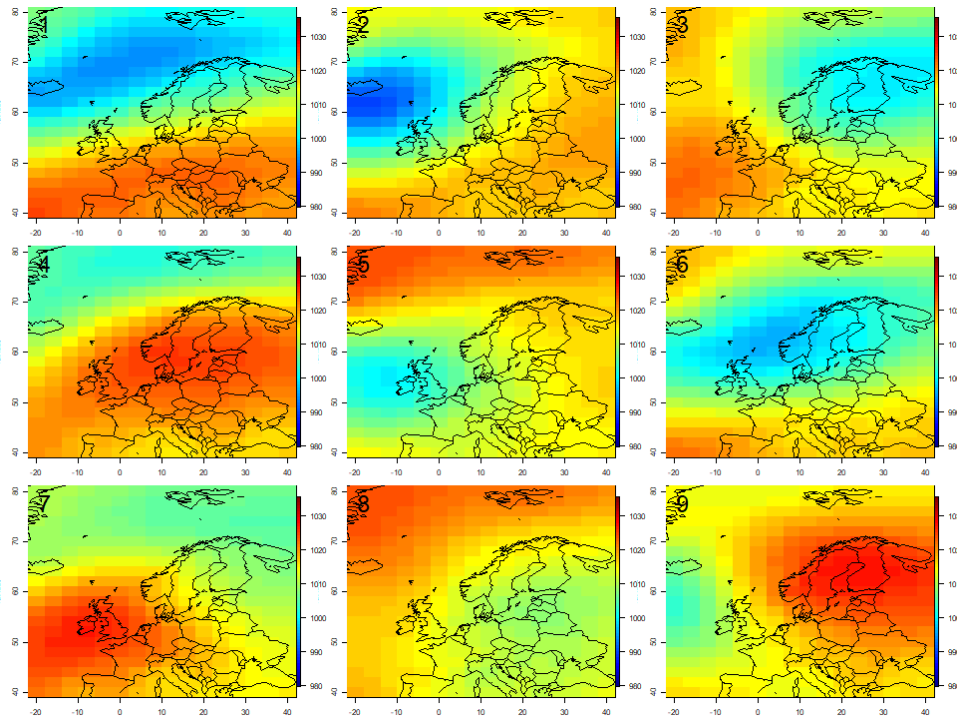


Figure A.4: 9 circulation types for Lund classification (LND09). First axis indicates longitude, while second axis indicates latitude. Colors are showing sea level pressure (SLP) in hPa. Red: high SLP, blue: low SLP.

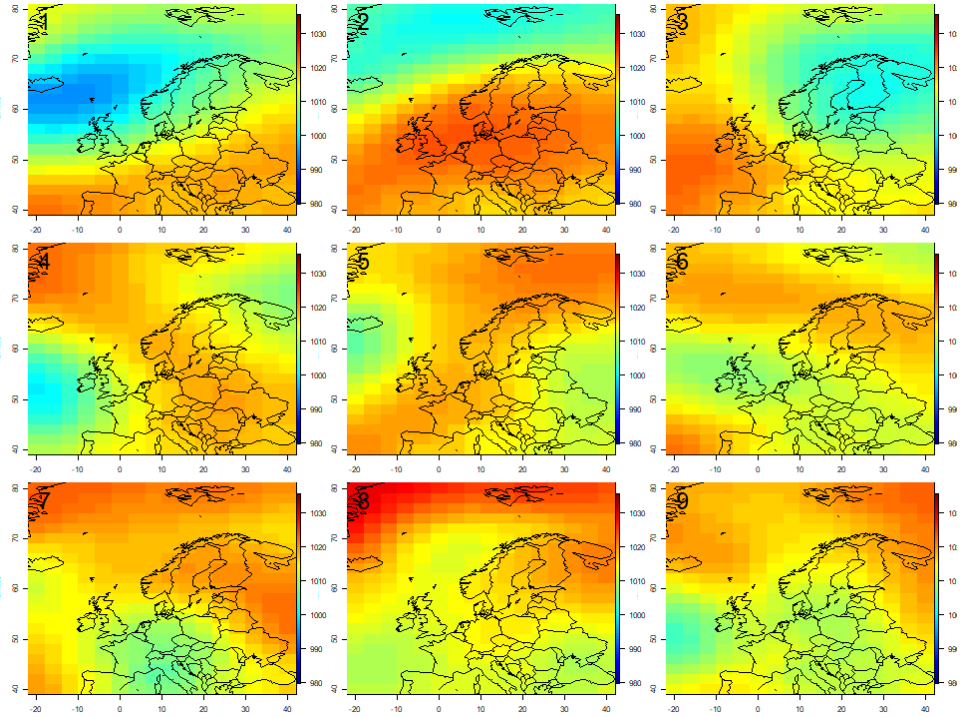


Figure A.5: 9 circulation types for PTT classification (PTT09). First axis indicates longitude, while second axis indicates latitude. Colors are showing sea level pressure (SLP) in hPa. Red: high SLP, blue: low SLP.

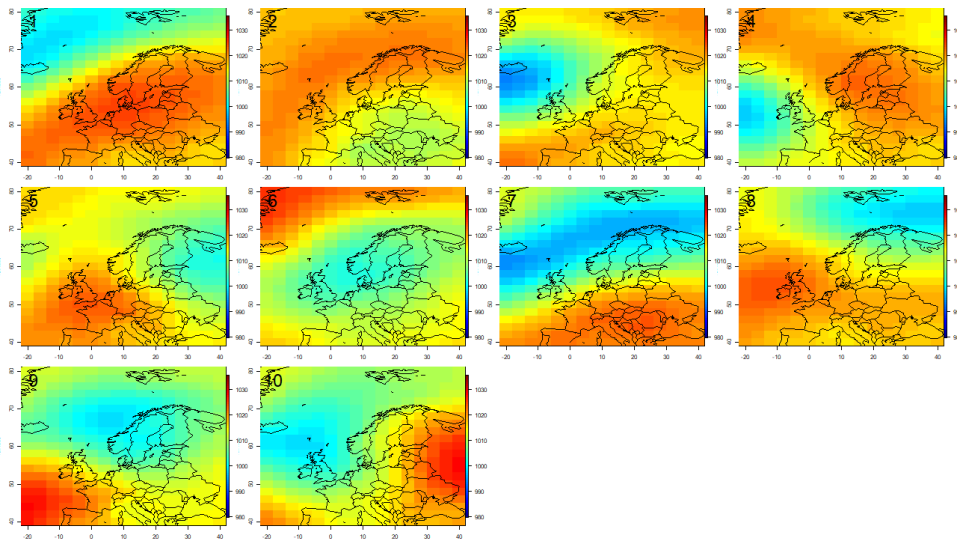


Figure A.6: 10 circulation types for PXE classification (PXE10). First axis indicates longitude, while second axis indicates latitude. Colors are showing sea level pressure (SLP) in hPa. Red: high SLP, blue: low SLP.

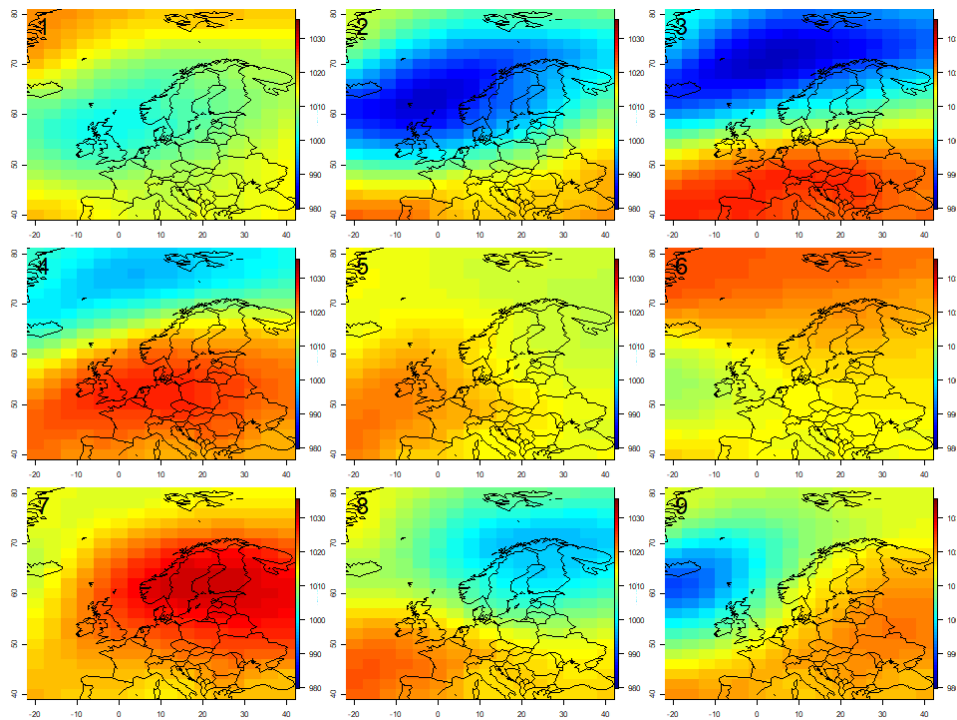


Figure A.7: 9 circulation types for simulated annealing clustering classification (SAN09). First axis indicates longitude, while second axis indicates latitude. Colors are showing sea level pressure (SLP) in hPa. Red: high SLP, blue: low SLP.

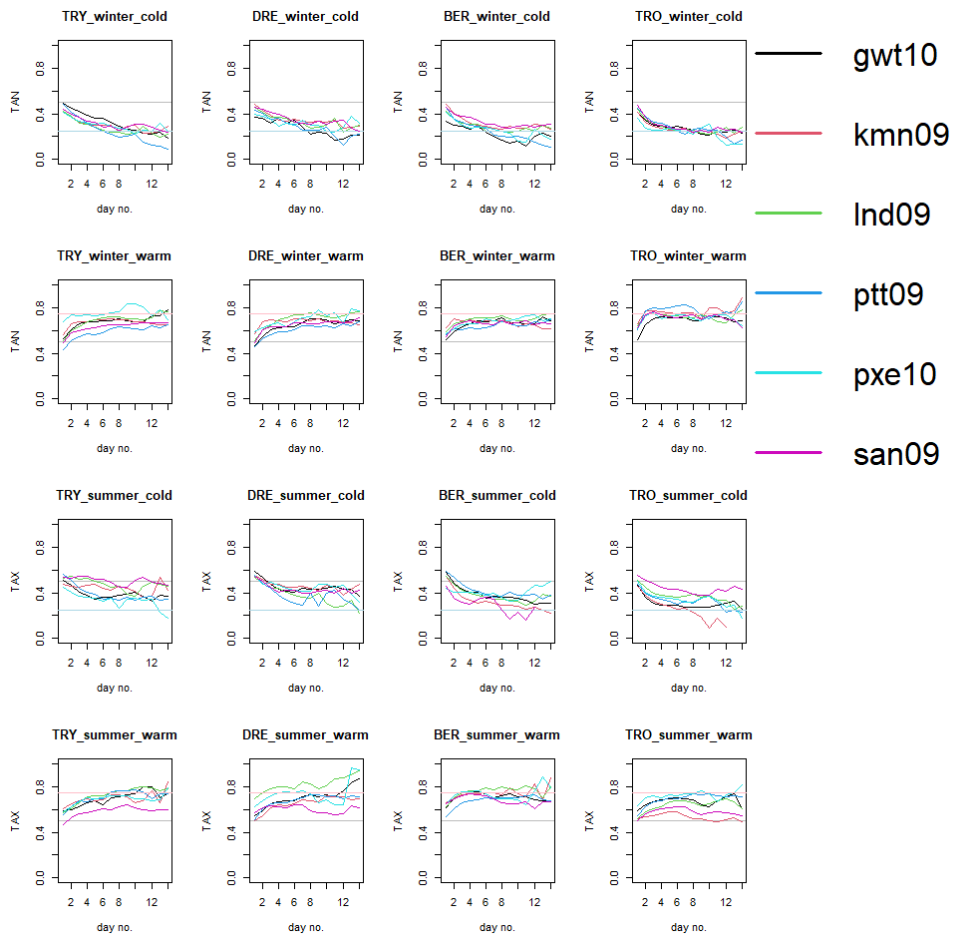


Figure A.8: Average temperature on each day of periods of persistent circulation based on CTs associated with each kind of spell. Horizontal lines are corresponding to the median temperature (gray), 25th percentile (light blue) and 75th percentile (light red).

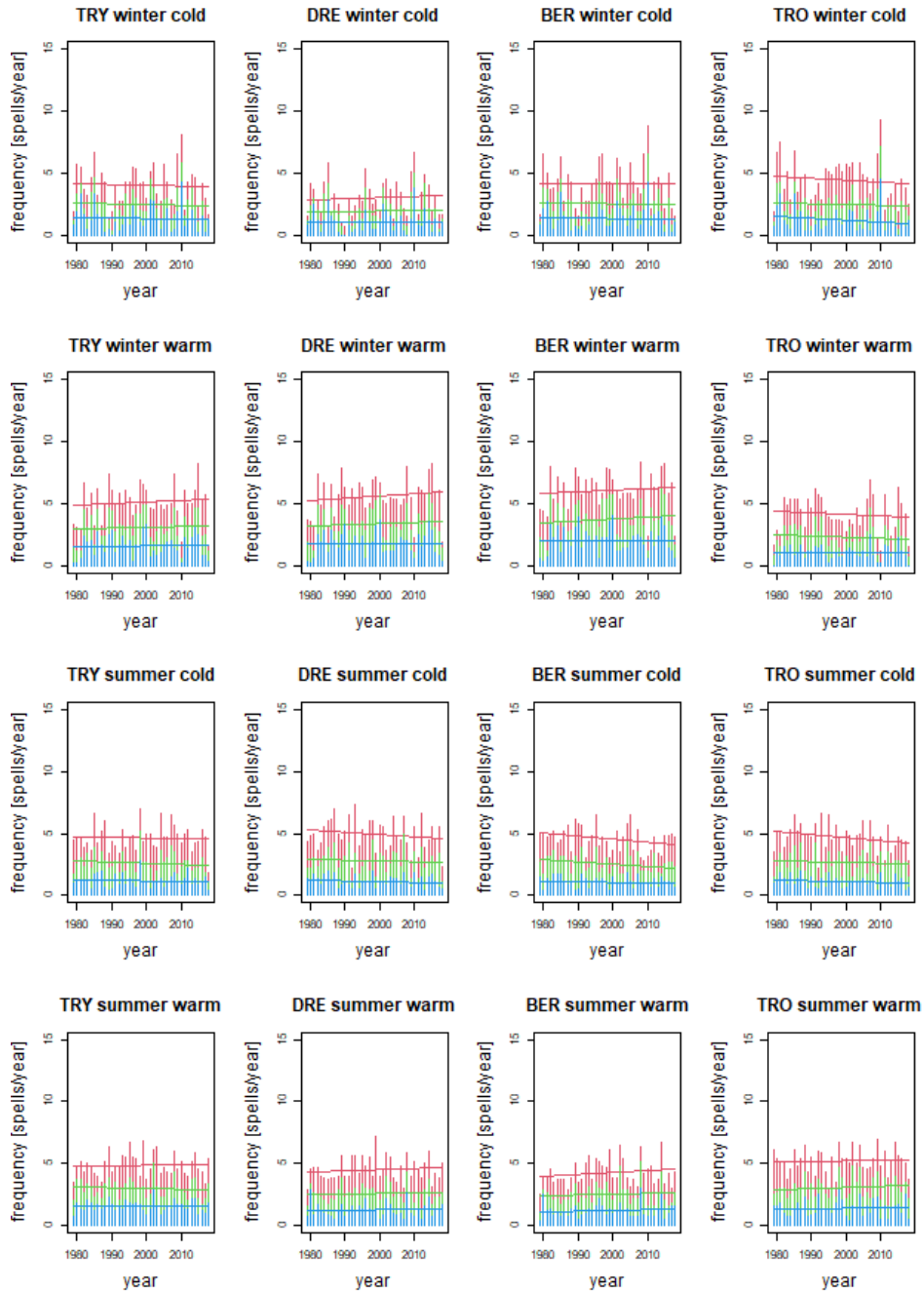


Figure A.9: Frequency of periods of persistent circulation resulting in cold and warm spells during winter and summer in four different locations as an average of all six classification methods. Vertical lines show number of periods for each year, while slanted lines show linear regression trends.